"REVIEWED"

# RESULTS OF THE 1989 EXPLORATORY CLOUD SEEDING EXPERIMENT IN ILLINOIS BASED ON SYNOPTIC WEATHER CONDITIONS

N. E. Westcott, S.A. Changnon, Jr., R.R. Czys,
R.W. Scott, and M.S. Petersen

Illinois State Water Survey
Atmospheric Sciences Division
Champaign, Illinois

ABSTRACT. The 1989 Illinois summertime cloud seeding results have been examined in the context of synoptic weather conditions. It was found that six of the 12 experimental units occurred under cold-front conditions, and four units under air-mass conditions when no kinematic trigger was obvious. When cold fronts were present, the tallest daily echo tops, the highest first echoes, the strongest updrafts, and hail were observed. While deep convection occurred on both types of days, a larger amount of potential buoyancy was available and stronger vertical shear was present on cold-front days.

Sixty echo cores treated near cloud top with silver iodide (AgI) or sand flares were examined before, at, and after treatment. It was expected that the cold-front cores would be larger than the air-mass cores. Instead, the air-mass cores in the mean were older, larger, more reflective, and contained more liquid water and a larger fraction of ice than the cold-front cores. The cold-front cores had a broad distribution in vertical motion as estimated by both aircraft and radar. This same broad distribution also was observed in the maximum values of height, area, and reflectivity. There were many small cold-front cores and a few large ones. The cold-front cores with the largest and strongest updrafts grew the tallest. This relationship was much weaker for the air-mass cores. It was postulated that the smaller cores were more subject to the detrimental effects of entrainment on cold-front days. On the air-mass days, all tracked cores were already joined with another echo by the time of treatment. In this protected environment, less affected by vertical shear, even the smallest of the air-mass cores grew.

AgI/sand differences also were examined. For the cold-front cores, it was found that at treatment time, there was a disproportionate number of small AgI-treated cores, and the largest cores were treated with sand flares. The sand cores also had the largest pre-treatment and treatment time growth rates. No seeding effect could be deduced from the cold front sample because of this bias towards smaller AgI-treated cores. No such bias was observed for the air-mass cores. However, the air-mass sand-treated cores grew taller than the AgI-treated cores. Since cloud seeding was expected to lead to an increase in vertical growth, if seeding affected the growth of the individually treated cores, it was in a negative way for this small sub-sample of air-mass cores. However, in terms of core duration, maximum horizontal area and maximum reflectivity, the sand- and AgI-treated cores were similar. These data failed to confirm the earliest steps of the dynamic seeding hypothesis suggesting that silver iodide treatment invigorates individual cloud growth.

## 1. INTRODUCTION

A randomized cloud seeding experiment, the Precipitation Augmentation for Crops Experiment (PACE) was conducted in Illinois during the summer of 1989, to examine the early response of clouds to silver iodide (AgI) seeding. The experiment was designed around the dynamic seeding hypothesis, focusing on individual clouds within multi-celled cloud systems (Changnon et al., 1991). The first steps of the dynamic seeding hypothesis propose that cloud seeding should enhance the vertical growth of individual clouds through the release of latent heat by the rapid freezing of supercooled water. During the

1989 experiment, clouds within an experimental unit were treated with AgI or sand flares, just beneath cloud top (~ -10°C). Three-dimensional histories of the radar echo cores associated with these clouds and aircraft measurements made by the seeding aircraft have been used to examine the initial steps of the hypothesis.

Later steps in the hypothesis suggest that the horizontal extent of the cloud system may be enlarged through the initiation of new cells brought about by convergence resulting from invigorated downdrafts, leading to increased precipitation (Orville, 1986; Simpson, 1980). If a seeding effect as evidenced by increased echo top heights were observed within the first 20 minutes after cloud treatment, this information would be invaluable to the direction of future experimentation. While the later steps of the hypothesis have not been addressed here, such confirmation also would lend credence to results which suggest an effect on larger storm scales.

The objective of this study is to present the results of the 1989 cloud seeding experiment in the context of synoptic weather conditions. This has been done for several reasons. As in past cloud modification projects, partitioning the data into groups collected during similar weather conditions should reduce the natural day-to-day variability of cloud behavior, thus enlarging the chance to detect a seeding signal. Under different weather conditions, cloud growth characteristics may vary and treatment effects could differ. Cloud histories have been examined to determine whether significant differences in growth existed under different synoptic conditions. This approach provides a basis for the comparison of results with other projects conducted in the Midwest and elsewhere.

### 1.1. Use of synoptic variables in past experiments

Summertime convection occurs under many synoptic weather conditions in the Midwest. These conditions can be described in many ways: by synoptic types, by thermodynamic indexes, by wind field parameters, by cloud model runs, by cloud characteristics in the study area, or by a combination of the above. All of these methods have been used to forecast like conditions for cloud development and also in subsequent data analysis to help reduce the natural variability of cloud growth characteristics.

In cloud seeding experiments of relatively short duration, such as a single summer season, it is especially important to examine the ambient conditions under which clouds form. It is possible for seeded clouds to develop under conditions in which clouds are expected to be large, while nonseeded clouds could develop during periods when clouds are expected to be small. This occurred during the 1986 PACE field program (Westcott, 1990). The 1986 data were partitioned according to synoptic weather conditions during the analysis phase. As a result, clouds were segregated into categories of like behavior, drastically changing the interpretation of the 1986 seeding results. The time of day, type of forcing, amount of cloud cover, and first echo height were important in describing the different weather conditions.

Cloud modification projects relevant to the Midwest have partitioned their data according to various atmospheric conditions. During Project Whitetop, a cloud seeding experiment in south- central Missouri (1960-1964), precipitable water and wind direction were used to forecast acceptable days for treatment. In the analysis of the Whitetop results, wind direction (defined by the seeding plume motion), wind speed at 1.2 km above mean sea level (MSL), the presence of precipitation in the nonplume area, the number of seeding hours, and the maximum echo-top height were used as criteria to partition the days for analysis of cloud seeding effects on daily rainfall (Braham, 1966). A slightly positive seeding effect was found on days with maximum echo tops of 6 to 12 km and on days with west winds. A negative treatment effect was observed on days with south winds, and a stronger negative effect was found on days with maximum echo tops of more than 12 km. On days with precipitation in the control area, modest increases in statistical significance were found for these positive and negative effects. When more seeding material was applied, the mean rainfall in the target area decreased, suggesting that overseeding had occurred. No effect was observed on dry days with maximum echo tops of less than 6 km (Flueck, 1971; Braham, 1979).

Two major inadvertent cloud modification projects of the 1970s examined summer rain periods in and around St. Louis (the METROMEX project) and Chicago. The rain events covered in METROMEX (1971-1975) were partitioned by synoptic weather type, wind direction, and amount of precipitation (Vogel, 1977; Changnon, 1978a; Braham, 1981). The Chicago Hydrometeorological Area Project (CHAP, 1976-1979) employed the same stratification criteria (Changnon, 1980). The duration, areal coverage, and total rainfall amounts were found to vary according to synoptic type.

In the Rapid Project and the North Dakota Pilot Project (NDPP), both cloud seeding experiments in the Dakotas (1964-1966; and 1969-1972, respectively), precipitable water, 850 -millibar (mb) wind conditions, and vorticity advection were used to forecast suitable rain periods for seeding (Dennis and Koscielski, 1969; Dennis et al., 1975). Both projects partitioned their results according to storm type (shower and storm days). The Rapid Project data also were stratified by direction of flow. The NDPP seeding results were examined in terms of the 500-mb temperature, cloud-base temperature, and cloud model-derived seedability. The Rapid Project results indicated increased daily rainfall on the shower days and a negative treatment effect on the storm (squall line) days with flow from the NW. The NDPP results indicated a slightly positive seeding effect on both types of days. In addition, first echoes were observed to form at a lower height on seeded days (Dennis and Koscielski, 1972).

## 1.2. Elements leading to the design of the 1989 experiment

The 1986 and 1989 field experiments were both designed with the intent of deriving the largest possible sample of experimental units. In planning the 1986 seeding experiment in Illinois, the randomization of the treated rain periods (areas) was to be based on synoptic type. But unlike the multiyear projects mentioned previously, it was reasoned that a single six-week project might produce too few samples in each category. Thus, no blocking was done (Changnon et al., 1987), and the clouds were simply randomized based on rain periods. Each rain period had to be separated by an hour or more from other rain periods. The analysis of the three 1986 experimental units revealed the possibility of more than one discrete rain area for seeding within the rain periods.

In the 1989 experiment, the randomization was designed on a more localized scale, following the concept of the Southwest Texas Project (Rosenfeld and Woodley, 1989). An experimental unit was defined as a moving circle with a radius of 28 km, containing one or more echoes. The circle was defined by centering on the geometric mean of the treated cores. A mean unit motion was determined from the center of the unit at the time of the last treatment and its subsequent locations as noted in real time. The experimental unit's movement was then calculated by interpolating its position backward and forward in time. Only one type of treatment was applied to the echoes within an experimental unit, and none was applied in the 28-km buffer zone surrounding each unit. During the 1989 experiment, two or more large cloud experimental units occurred during a given convective period on three days. Thus, the experimental design was successful in increasing the number of experimental units over the number that would have been obtained using the 1986 rules.

The PACE 1986 data were examined for criteria that might be useful in predicting convection suitable for modification in 1989. This was done in two ways, first using five standard thermodynamic criteria (Scott and Huff, 1987); and secondly, using a combination of the temperature of the convective condensation level and the potential buoyancy (Scott and Czys, 1992). These parameters were useful in indicating the probability of convective potential (categorize the maximum daily echo-top height as short, medium, or tall).

The results of PACE 1986, and projects Whitetop and METROMEX suggested that the expected daily echo-top height was the appropriate blocking parameter for the 1989 experiment. A climatology of daily maximum echo tops was determined from METROMEX and revealed a bimodal distribution of echo-top heights in rural storms (Braham and Wilson, 1978; Braham, 1981). The major inflection point in the distribution was at 10 km, with peaks at 6 and 12 km. A seeding response would be especially difficult to detect and actually might differ for events when clouds typically reached 6 to 10 km, or when they grew to 12 km or higher. Thus, to maintain the largest possible sample of clouds within each randomized group, only two randomization blocks were used, based on cloud-top heights observed at the time the experimental unit was declared: 1) The large cloud experimental units were those in which clouds were actively growing through the flight level about 5.5 km above ground level (AGL) at about -10°C, while other cloud tops in the area were exceeding 9 km. 2) The small cloud units were ones in which clouds were just reaching the flight level (6 to 8 km).

The synoptic characteristics, and in particular the thermodynamic indices were found to be very different for the large and small cloud units in 1989. The large clouds units contained clouds with the greatest growth, and the units were the largest rain producers. Thus, the 12 large cloud experimental units are the focal point of our study.

The randomization procedure successfully provided a balanced number of AgI- and sand- treated units and clouds. Six of the 12 large cloud experimental units were treated with AgI and six with sand for a total of 35 AgI-treated echo cores and 32 sand-treated echo cores.

Within the large cloud group, however, two distinct cloud populations were sampled based on synoptic weather conditions. These two populations of clouds were classified as "cold front" and "air mass", although various other synoptic characteristics could typify these days. The cloud data from 1989 were thus partitioned and analyzed based on these synoptic groupings.

# 2. DATA AND ANALYSIS

## 2.1. Radar echo data

The primary data for evaluation of 1989 cloud seeding results are reflectivity data collected using the CHILL 10-cm radar. A minimum reflectivity threshold of 10 dBZ was imposed on the analyzed data. The radar volumes were of 1.5- to 4-min durations, and the echo cores were located within 30 to 110 km of the radar. The data were interpolated to a grid encompassing the experimental unit. The 1989 study focused on the early growth characteristics of individual cores, which in most cases merged with a multicelled cloud system. An interactive core tracking program (ICORT) was developed for use with the three-dimensional interpolated reflectivity data (1 x 1 x 1 km resolution).

An echo core was defined as an identifiable maximum in reflectivity. Merging was determined to occur when a core became part of a multicored system. Nearly all of the echo cores were merged with other echoes at some point in their history. The only ones not merging had very short lifetimes. The echo

cores at the time of first detection were classified as isolated, loosely joined, or strongly merged. For the loosely joined cores, a distinct core was observable at all heights, and typically they were joined at a single level. The lowest levels of each of the strongly merged cores were not distinct from their parent storms at the time of first detection, but they could be identified at low levels later in their history.

This breakdown of first echoes basically stratified the echo cores by the distance of separation of new feeder clouds from the parent storm. Of the treated cores, the isolated cores typically formed within 5 km of another echo, and the loosely joined clouds about 1 km from an adjacent core, according to the resolution of the radar interpolation scheme. The strongly merged cores may be reminiscent of the weak evolution observed by Petersen (1984) and Westcott and Kennedy (1989), where the downdraft-induced outflow was so close to the existing echo in a multicelled storm under weak shear conditions, that as a result, the new core appeared as a bulge on the edge of the parent storm, and only became a distinct core later in its history.

The simpler cores generally followed a pattern of 1) formation at a height of 3 to 6 km, 2) vertical, and horizontal expansion, and 3) descent of the echo core toward the surface. The expansion of the core and the drop in the altitude of its maximum reflectivity core often occurred simultaneously. The same growth model was found in the mid to upper levels for the more complex merged cores, and that pattern was assumed in making the more subjective decisions on defining the beginning and ending of the cores at the lower levels. Echo cores were tracked until they dissipated or until they became indistinguishable from an adjoining echo. For about 1/3 of the cores, tracking ceased near the time when they reached their maximum values in area, height and reflectivity, when the cores could no longer be distinguished from other echo. Tracking was terminated on about 2/3 of the cores either because they dissipated or lost their identity well into their dissipation stage. Reflectivity contour intervals of 2.5 dBZ were used. Sixty-seven echo cores were tracked, and four additional clouds that were treated but never echoed.

Various echo-core properties were determined for the individual cores at the time of first echo, at the time of treatment, and at the times of the maximum in height, area, and reflectivity. The amount of change and the rate of change of these properties were computed between the time of first echo and the time of treatment; and between the time of treatment and the first time when the maximum height, area, or reflectivity were attained. The duration of the echo core was estimated as the time from first echo to the time of maximum area. Area was chosen as a basis for the period of growth because the core area typically continued to expand after the maximum height was reached (Westcott, 1990). This estimate likely underestimates core durations, but in a uniform manner. On average, tracking continued 10 minutes beyond the time when the maximum area was reached.

Additionally, computations of vertical growth of the echo cores were made 2 minutes prior to treatment, at the time of treatment and 4 minutes after treatment by fitting a polynomial to the 10-dBZ contour defining the echo top. Some values were missing in the vertical growth parameters, because some cores did not echo until after treatment, some dissipated so rapidly that not enough data were available, and a few cores were poorly fit by the computer scheme. Definitions of echo-core properties employed in this study are described in the Appendix and in Czys et al., (1993).

The properties of other echoes in addition to the treated ones have been employed to characterize convection within the units. Earlier projects, in particular Project Whitetop and the Florida Area Cumulus Experiment (FACE), found important covariates in the amount and duration of echo coverage or rainfall prior to treatment (Simpson and Woodley, 1971; Biondini et al., 1977) and in the rainfall in areas adjacent to the target area during and after treatment (Braham, 1966). In this analysis, the radar-estimated rainfall was computed for reflectivities $\geq$ 30 dBZ over a 240 x 240 km area centered on the radar site near Champaign (CMI), and also for the area encompassing the experimental unit. Rainfall totals were accumulated from 15 minutes prior to treatment to treatment, from the beginning to the end of treatment, and in 15-minute periods after the last treatment pass. The maximum echo top observed within the unit and the maximum daily echo top also were determined.

First echo information was gathered on all of the isolated echoes within and nearby each experimental unit. These data were grouped according to whether they occurred before or after the first treatment and whether they formed inside or outside the experimental unit. They were used 1) as an indicator of cloud growth properties, 2) to corroborate the first echo properties from the smaller population of treated clouds, and 3) as a point of comparison for projects in other locations.

### 2.2. Cloud updraft properties at time of treatment

During PACE 1989, an aircraft outfitted with microphysical instrumentation was used both to seed clouds at about the -10°C altitude and also to sample the microphysical, thermodynamic, and kinematic properties of the updraft region of the treated cloud (Changnon et al., 1991; Czys et al., 1992). The updraft properties of each cloud were examined to confirm cloud conditions detected by radar.

### 2.3. Weather forecast parameters

The synoptic variables were computed from the 0700 central daylight time (CDT) Peoria (PIA) soundings. Peoria is located about 130 km northwest

of CMI and is on the edge of the experimental area. Forecasting studies have indicated that the early-morning PIA soundings are useful for predicting convective conditions in the PACE target area (Scott and Czys, 1992; Scott and Huff, 1987). These same variables were computed for the 1900 CDT soundings, but many of these soundings were disturbed by daytime convection and thus were difficult to assess. An NCAR CLASS sounding unit was operated at CMI, and soundings typically were made at midday. Due to mechanical/electrical problems, rawinsonde data was limited to morning soundings for days in late July. However, when possible, the afternoons soundings were used to determine if conditions had changed significantly from the 0700 PIA sounding values.

## 3. WEATHER CONDITIONS

### 3.1. Synoptic weather classifications

Generally, the largest rain-producing systems in the Midwest occur when a kinematic triggering mechanism initiates the convection. Convection without any apparent large-scale forcing, the so-called air-mass storms are common also. Definition of the type of forcing associated with each experimental unit was based on a classification scheme for these synoptic triggering mechanisms that was developed during METROMEX (Table 1).

Many of the 1989 large cloud experimental units occurred with two synoptic conditions: six units were categorized as cold frontal and four units as air mass. The other two units were classified as a squall zone and an upper level, low-pressure system. These two units both occurred on days when a second experimental unit had been declared as a small cloud unit. The PIA 0700 CDT sounding data on these days reflected some weather conditions conducive to large clouds (Table 2), and some common to small cloud systems (Table 3).

Cold fronts are a common type of forcing in the central Midwest, particularly in the spring and early summer (Hiser, 1956; Vogel, 1977; Changnon, 1980). The six experimental units classified as cold fronts and occurred on four days, in May, June, and early July. During two of the units, cold fronts were moving so slowly that they could have been classified as stationary fronts.

Air-mass storms occur more often in the summer and are generally smaller in area and duration than cold-front storms (Hiser, 1956). Earlier research has shown that air-mass storms make up only 7 to 33% of the total number of storms in various Midwest regions, and they contribute only about 0.5 to 20% of the total rainfall (Changnon, 1980; Vogel, 1977; Hiser, 1956; Hudson et al., 1952). While air-mass storms are generally smaller in overall rainfall production, their relative importance has been found to increase during dry years (Huff, 1969). Cold-front rain events typically make up a higher percentage of the total number of summer rain periods (15 to 40%) and produce 12 to 40% of the total rainfall. However, only about 50% of the cold-front storms occur during daylight hours, when air-mass storms are at their peak and when cloud seeding is usually undertaken. Air-mass storms also occur at a time in the growing season when rainfall increases due to cloud seeding would be most beneficial. During METROMEX, hail was observed on both air-mass and cold-front days although it was more common on cold-front days. Hail occurred during 23% of the cold-front periods and during only 3% of the air-mass periods (Changnon, 1977).

Table 1. Synoptic Classifications (after Vogel, 1977)

| |
|---|
| Squall Line Rain Events: |
| A non-frontal group of thunderstorms accompanied by a trigger mechanism, usually a short wave trough. The convective activity associated with the storm system is intense, well-organized, and often times arrayed in a narrow band or line of active thunderstorms. **(0 events in 1989)** |
| Squall Zone Rain Events: |
| A mesoscale system of thunderstorms organized into an area or cluster and independent of a frontal zone. These storms, like squall lines, tend to move across large regions of the Midwest and an upper-air impulse is usually discernible. (1 event in 1989) |
| Frontal Rain Events: |
| Precipitation forms within 120 km of a surface front (cold, static or warm). There is no synoptic evidence that this precipitation is associated with a squall zone which on occasion moves 40 km or more ahead of a front. (6 events in 1989) |
| Pre-Frontal and Post-Frontal Rain Events: |
| Precipitation associated with a frontal structure but at a distance of 120 to 140 km ahead or behind a front. (0 events in 1989) |
| Air Mass Rain Events: |
| A shower or thunderstorm generated within an unstable air mass. No large scale or mesoscale synoptic causes are evident. The resulting convective activity is usually widely scattered to scattered and weak. (4 events in 1989) |
| Upper Level Low Pressure Rain Events: |
| A cyclonic storm situated so close to the research area that it is not possible to associate the precipitation with a frontal or mesoscale weather structure. (1 event in 1989) |

Table 1 also lists four other types of summer rain-producing conditions, which were either not sampled or were characteristic of only one rainstorm. These represent about 55% of all summer events and produce 60% of all the rainfall (Vogel, 1977). Hence,

the two categories considered here, cold front and air mass, represent less than half of the potential rainfall conditions. In addition, the four air-mass units occurred on three consecutive days in late July and originated from a common air mass. Caution should be used in extrapolating these data to all instances of air-mass storms.

3.2. Meteorological conditions sampled in 1989

Thermodynamic and kinematic parameters depicting the environmental conditions observed during the 1989 experimental days, and a brief description of the observed storms are presented for each experimental unit (Tables 2-5). These environmental parameters chosen have been found by earlier studies to be related to the presence and intensity of convection. Two estimates of buoyancy were computed: the convective available potential energy (CAPE), and potential buoyancy (PB). CAPE was evaluated from cloud base to the top of the positive area (between the sounding and a representative moist adiabat on a skew-t diagram). It serves as an estimate of the net work per unit mass done by the environment on an air parcel (energy per unit mass gained by the parcel), that rises from the cloud base to the lowest level of zero potential energy. Thus, CAPE is a measure of potential instability at middle and upper levels (Montcrieff and Green, 1972; Weisman and Klemp, 1982, 1984; LeMone, 1989; Bluestein and Jain, 1985).

PB was computed as the difference between the pseudoadiabat through the cloud base (estimated by the CCL) and the environmental temperature at 500 mb, the approximate treatment level. Thus PB is related to the average updraft from cloud base to 500 mb (Mather et al., 1986). LeMone (1989) found that in the absence of other external forcing, CAPE is related to the cloud's vertical velocity and potentially to the cloud's depth. Both CAPE and PB were found to be larger for the cold-front days. Although there was external forcing on the cold-frontal days, the estimates of CAPE and PB suggest that in the absence of the forcing, stronger updrafts and taller clouds might still be expected during these periods.

The lifted index (LI), which is often used as a severe weather forecast parameter is similar in definition to PB. LI was computed by lifting a parcel along the moist adiabat from the lifted condensation level to 500 mb, where the temperature, considered to be the updraft temperature of a developing cloud, is compared to that of the environment (Peppler, 1988). As found with PB and CAPE, the LI was greatly different for cold-front units, air-mass units (Table 2), and small cloud units (Table 4).

Cold-front and air-mass days also were contrasted according to the prevailing winds. Winds on the cold-front days were typically from the west, and on the air-mass days from the south (Table 2). The vertical shear of the horizontal wind was computed in two ways. First it was computed for the bulk Richardson number (Table 2), as the difference between the density-weighted mean wind through 6 km and the mean wind within a representative surface layer (500 m) wind (Weisman and Klemp, 1984). Seasonal variation in shear was pronounced, with progressively less shear present later in the convective season, as would be expected from the northward retreat of the polar front. The cold-front soundings showed somewhat stronger shear than the air-mass days, particularly in May and June. The afternoon PIA and CMI soundings indicated shear values of more than 10 $m^2s^{-2}$ on the cold-front days, but no increase of shear during the afternoon on the air- mass days (Table 2). Many studies have indicated that shear is necessary for the development of severe storms (e.g., Marwitz, 1972; Weisman and Klemp, 1982; Fovell and Ogura, 1989).

More recently, the interaction of low-level shear with the cold surface outflow has been found to be important in the development of long-lived squall lines (Rotunno et al., 1988; Weisman et al., 1988). The low-level shear at 0700 CDT on three of the four cold-front days was stronger than on the air-mass days (Table 3), even though the shear was of moderate intensity on some days. From the above discussion of the ambient weather conditions, one might expect the development of large clouds and possibly severe weather on cold-front days, as opposed to air-mass days. In fact, 16-km echo tops and hail were observed in the 150-km-radius target area during the afternoon and early evening hours on each of the four cold-front days.

The height and temperature of the first echo formation on the cold-front and air-mass days also indicated differences in storm and precipitation growth (Table 3). The cloud-base temperatures as estimated by the temperature of the convective condensation level (TCCL), typically were warmer on the air-mass days than cold-front days. The precipitable water (PW) also was greater for air-mass days. In this warmer and moister environment, first echoes could and did form at lower altitudes on the air-mass days. The first echo heights on cold-front days were higher and colder (Table 3) with 16% forming above the freezing level, 33% below the freezing level, and 51% straddling the zero degree isotherm. First echoes on air-mass days formed completely below the freezing level (51%) or straddled it (49%), but none formed completely above the freezing level. The higher first echoes may indicate that raindrops took longer to form in an atmosphere with somewhat less moisture available, that the coalescence process was more active on the air-mass days, or that the updraft strength at the time of first echo was greater on cold-front days.

Other indices indicated that while more intense convection might be expected on the cold-front days, clouds could reach 12-km during air-mass days as well. The bulk Richardson number (Ri) for the air-mass and cold-front days indicated that convection was favored on all large cloud type days. Also, a relationship among PB, the TCCL, PW and the maximum daily cloud-top height developed by Scott

Table 2. Large cloud experimental unit weather indices. All parameters were computed from the 0700 CDT PIA soundings. The means (above) and standard deviations (below) are provided for the cold front air mass units; only the mean is computed for the other synoptic category. The a and s refer to AgI and Sand treatments.

| ExpU Cloud Type | Date | Synoptic Type | CAPE $m^2s^{-2}$ | Vert Shear $m^2s^{-2}$ | Ri | TCCL °C | Ppt Water °C | PB °C | LI °C | Ki °C | MKi °C | Jeff °C | MSh °C | SWT °C |
|---|---|---|---|---|---|---|---|---|---|---|---|---|---|---|
| Cold Front Experimental Units | | | 852 | 11.9 | 82.5 | 15.9 | 3.7 | 6.7 | -4.6 | 32.1 | 41.9 | 33.7 | 7.6 | 226 |
| | | | 354 | 6.7 | 50.1 | 1.9 | 0.5 | 1.8 | 4.3 | 3.9 | 3.1 | 4.7 | 3.0 | 125 |
| 5 a | 6-01-89 | cold frt | 1339 | 25.0 | 53.5 | 18.0 | 4.4 | 6.4 | -5.3 | 38.1 | 43.3 | 37.2 | 5.3 | 298.7 |
| 11 a | 6-23-89 | cold frt | 636 | 11.7 | 53.2 | 15.8 | 3.1 | 5.0 | -2.1 | 24.8 | 30.8 | 32.9 | 10.7 | 166.5 |
| 13 s | 6-23-89 | cold frt | 636 | 11.7 | 53.2 | 15.8 | 3.1 | 5.0 | -2.1 | 24.8 | 30.8 | 32.9 | 10.7 | 166.5 |
| 17 s | 7-08-89 | cold frt | 613 | 8.0 | 76.5 | 13.8 | 3.8 | 8.2 | -3.8 | 30.6 | 31.6 | 39.3 | 8.1 | 356.6 |
| 18 a | 7-08-89 | cold frt | 613 | 8.0 | 76.5 | 13.8 | 3.8 | 8.2 | -3.8 | 20.6 | 31.6 | 39.3 | 8.1 | 356.6 |
| 19 a | 7-11-89 | cold frt | 1278 | 7.0 | 182 | 17.9 | 3.9 | 7.4 | -5.4 | 30.8 | 36.8 | 36.0 | 9.1 | 237.5 |
| Air Mass Experimental Units | | | 540 | 6.5 | 83.5 | 18.0 | 4.2 | 3.6 | -3.3 | 35.0 | 44.9 | 32.7 | 8.0 | 173 |
| | | | 57 | 0.4 | 13.7 | 1.2 | 0.8 | 0.1 | 0.5 | 1.7 | 0.6 | 1.5 | 0.3 | 20 |
| 22 a | 7-23-89 | air mass | 475 | 7.0 | 68 | 16.2 | 4.1 | 3.6 | -1.9 | 28.0 | 34.2 | 30.0 | 11.6 | 119.7 |
| 23 s | 7-24-89 | air mass | 510 | 6.7 | 76 | 18.3 | 4.1 | 3.4 | -2.4 | 30.2 | 36.3 | 33.1 | 10.4 | 180.7 |
| 24 s | 7-25-89 | air mass | 588 | 6.2 | 95 | 18.8 | 4.8 | 3.6 | -2.5 | 36.4 | 41.6 | 33.9 | 6.5 | 184.5 |
| 25 a | 7-25-89 | air mass | 588 | 6.2 | 95 | 18.8 | 4.8 | | -2.5 | 36.4 | 41.6 | 33.9 | 6.5 | 184.5 |
| Other Synoptic Type Experimental Units | | | 108 | 26.5 | 14.1 | 14.6 | 3.5 | 1.6 | -0.7 | 34.7 | 40.6 | 33.3 | 8.2 | 166 |
| 2 s | 5-19-89 | Sql Z | 10 | 45.6 | .2 | 13.2 | 3.3 | 0.8 | 0.3 | 33.8 | 40.1 | 32.9 | 8.5 | 180.9 |
| 20 s | 7-19-88 | LP | 206 | 7.4 | 28 | 15.8 | 3.7 | 2.3 | -1.6 | 35.5 | 41.2 | 33.6 | 7.8 | 151.9 |

Vertical shear computed from the PIA1900 CDT and the CLASS soundings.

PIA: 6-23-89: 13 $m^2$-$s^{-2}$; 7-08-89; 12 $m^2$-$s^{-2}$; 7-11-89: 12 $m^2$-$s^{-2}$,

CMI: 6-23-89: 22$m^2$-$s^{-2}$; 7-08-89: 11 $m^2$-$s^{-2}$; 7-11-89: 11 $m^2$-$s^{-2}$

PIA: 7-23-89: 7 $m^2$-$s^{-2}$; 7-224-89: 7-$m^2$-$s^{-2}$; 7-25-89: 6 $m^2$-$s^{-2}$.

Table 3. Large cloud experimental unit storm descriptors. The mean (above) and standard deviation (below) are provided for the cold front and air mass units. Only the mean is computed for the other storm types.

- Wind data are from the 0700 cdt PIA soundings;
- Mean first echo top height (km) and temperature (C) nearby and in the Experimental Unit (EU) both before and after treatment;
- Presence of hail in an extended network (EN: within 150 km of CMI);
- Max top height for the EU during the period of treatment, and for the afternoon for the EN (within 150 km of CMI);
-The storm type: line, area or isolated;
-The experimental unit (EU) and extended network (EN: a 240 x 240 km area centered on CMI) radar estimated rainfall (RER) accumulated from 15 min prior to the beginning of treatment to 15 min following the end of treatment.

| ExpU | Date | Sfc to 700 mb Shear deg. $ms^{-1}$ | 500 mb Winds deg. $ms^{-1}$ | Storm Motion deg. $ms^{-1}$ | FE Top Height km | FE Top Temp. °C | FE Sample | Hail | Max Top Height EU km | Max Top Height EN km | Storm Type | RER EU $10^4m^3$ | RER EN $10^6m^3$ |
|---|---|---|---|---|---|---|---|---|---|---|---|---|---|
| Cold Front Experimental Units | | | | | 5.7 | -8.90 | | | 14.5 | 16.6 | | 255 | 47 |
| | | | | | 1.3 | 8.3 | | | 1.4 | 0.5 | | 194 | 43 |
| 5 | 6-01-89 | 250 at 12 | 230 at 20 | 249 at 15 | 4.4 | -2.2 | 28 | Yes | 14.5 | 16.0 | line | 405 | 60 |
| 11 | 6-23-89 | 189 at 9 | 205 at 12 | 270 at 9 | 4.3 | -0.3 | 35 | Yes | 14.5 | 16.5 | area | - | - |
| 13 | 6-23-89 | 189 at 9 | 205 at 12 | 261 at 7 | 5.2 | -5.4 | 37 | Yes | 15.5 | 16.5 | line | 233 | 53 |
| 17 | 7-08-89 | 289 at 10 | 340 at 14 | 321 at 10 | 7.1 | -19.3 | 17 | Yes | 13.5 | 16.5 | isol | 82 | 53 |
| 18 | 7-08-89 | 289 at 10 | 340 at 14 | 314 at 10 | 7.4 | -19.0 | 11 | Yes | 16.5 | 16.5 | line | 497 | 109 |
| 19 | 7-11-89 | 224 at 5 | 230 at 9 | 282 at 4 | 5.7 | -7.0 | 32 | Yes | 12.5 | 17.5 | area | 58 | 7 |
| Air Mass Experimental Units | | | | | 3.8 | 3.8 | | | 13.3 | 13.8 | | 93 | 13 |
| | | | | | 0.5 | 4.0 | | | 1.0 | 0.5 | | 86 | 7 |
| 22 | 7-23-89 | 187 at 5 | 175 at 12 | 173 at 9 | 4.2 | -0.7 | 14 | No | 13.5 | 13.5 | line | 206 | 20 |
| 23 | 7-24-89 | 193 at 6 | 190 at 11 | 158 at 8 | 3.8 | 3.0 | 10 | No | 14.5 | 14.5 | area | 114 | 16 |
| 24 | 7-25-89 | 189 at 5 | 165 at 4 | 171 at 4 | 4.0 | 3.9 | 22 | No | 12.5 | 13.5 | area | 28 | 13 |
| 25 | 7-25-89 | 189 at 5 | 65 at 4 | 130 at 4 | 3.0 | 9.1 | 25 | No | 12.5 | 13.5 | area | 25 | 4 |
| Other Experimental Units (Days with large and small clouds) | | | | | 3.6 | -0.8 | | | 13.0 | 13.0 | | 162 | 127 |
| 2 | 5-19-89 | 202 at 19 | 180 at 23 | 235 at 15 | 3.0 | 1.8 | 5 | No | 11.5 | 11.5 | line | 146 | 156 |
| 20 | 7-19-89 | 240 at 5 | 265 at 8 | 280 at 7 | 4.2 | -3.3 | 17 | No | 14.5 | 14.5 | line | 177 | 97 |

Table 4. Small cloud experimental unit weather indices. All parameters were computed from 0700 CDT PIA soundings. The means (above) and standard deviations (below) are provided. AgI or sand treatments are indicated by a and s.

| ExpU Cloud Type | Date | Synoptic Type | CAPE $m^2s^{-2}$ | Vert Shear $m^2s^{-2}$ | Ri | TCCL °C | Ppt Water °C | PB °C | LI °C | Ki °C | MKi °C | Jeff °C | MSh °C | SWT °C |
|---|---|---|---|---|---|---|---|---|---|---|---|---|---|---|
| Experimental Units | | | 19 | 10.9 | 1.3 | 13.3 | 3.4 | 0.1 | 1.7 | 25.5 | 31.6 | 30.9 | 9.5 | 160 |
| | | | 47 | 5.0 | 3.2 | 2.4 | 0.6 | 0.9 | 1.2 | 12.0 | 11.6 | 1.1 | 1.2 | 35 |
| 6 s | 6-03-89 | cold frt | 11.5 | 14.6 | 7.9 | 9.1 | 2.4 | -.2 | 2.9 | 28.9 | 36.2 | 30.7 | 8.8 | 212.9 |
| 8 a | 6-12-89 | Sql Z | 0 | 14.3 | 0 | 15.6 | 3.8 | -.6 | 0.8 | 33.9 | 39.7 | 32.0 | 8.6 | 164.6 |
| 9 s | 6-12-89 | Sql Z | 0 | 14.3 | 0 | 15.6 | 3.8 | -.6 | 0.8 | 33.9 | 39.7 | 32.0 | 8.6 | 164.6 |
| 14 s | 6-27-89 | cold frt | 0 | 11.5 | 0 | 12.9 | 3.7 | 0.1 | 2.6 | 27.4 | 32.5 | 30.9 | 9.6 | 156.5 |
| 15 a | 6-27-89 | cold frt | 0 | 11.5 | 0 | 12.9 | 3.7 | 0.1 | 2.6 | 27.4 | 32.5 | 30.9 | 9.6 | 156.5 |
| 16 s | 7-02-89 | LP | 0 | 9.4 | 0 | 13.5 | 2.8 | 1.8 | 0.2 | 1.8 | 8.7 | 29.1 | 11.8 | 103.5 |



Table 5. Small cloud experimental unit storm descriptors. The mean (above) and standard deviation (below) are provided.

| ExpU | Date | Sfc to 700 mb Shear deg. $ms^{-1}$ | 500 mb Winds deg. $ms^{-1}$ | Storm Motion deg. $ms^{-1}$ | FE Top Height km | FE Top Temp. °C | FE Sample | Hail | Max Top Height EU km | Max Top Height EN km | Storm Type | RER EU $10^4m^3$ | RER EN $10^6m^3$ |
|---|---|---|---|---|---|---|---|---|---|---|---|---|---|
| | | | | | 3.4 | 3.2 | | | 9.0 | 11.1 | | 57.2 | 13.4 |
| | | | | | 0.5 | 3.7 | | | 0.9 | 2.1 | | 26.5 | 9.0 |
| 6 | 6-03-89 | 155 at 13 | - | 271 at 17 | 3.9 | -2.3 | 15 | Yes | 10.5 | 11.5 | arca | 89.1 | 27.1 |
| 8 | 6-12-89 | 235 at 8 | 225 at 8 | 257 at 13 | 3.6 | 1.9 | 22 | No | 8.5 | 8.5 | bline | 40.2 | 6.6 |
| 9 | 6-12-89 | 235 at 8 | 225 at 8 | 260 at 14 | 3.3 | 3.4 | 13 | No | 8.5 | 8.5 | isol | 62.6 | 3.2 |
| 14 | 6-27-89 | 189 at 6 | 245 at 15 | 289 at 11 | 2.8 | 7.8 | 23 | No | 8.5 | 13.0 | isol | 16.9 | 8.2 |
| 15 | 6-27-89 | 189 at 6 | 245 at 15 | 306 at 9 | 2.9 | 6.9 | 23 | No | 10.5 | 13.0 | line | 80.5 | 17.9 |
| 16 | 7-02-89 | 158 at 2 | 160 at 2 | 96 at 4 | 3.9 | 1.7 | 25 | No | 8.5 | 12.0 | bline | 53.6 | 17.4 |

and Czys (1992) showed those days to have > 60% probability for forming tall clouds. The other synoptic types fell into the < 60% category.

Several other indices also signaled large storms on cold-front and air-mass days. The K index, the modified K index, the modified Showalter index, the Sweat index, and the Jefferson index have been found to be correlated with rainfall in the midwest (Peppler and Lamb, 1989), Scott and Huff (1987) found that if four out of five of these indices exceeded a critical value at both PIA and Salem, IL, (SLO) at 0700 CDT, deep convection would likely occur in the target area. Except on 23 June 1989, the 0700 CDT PIA soundings alone (SLO was no longer in existence in 1989) indicated that deep convection could occur.

On the two days that were not classified as cold-front or air-mass, a second unit was classed as a small cloud unit. The morning sounding on 19 May and 19 July 1989, indicated that CAPE and PB were quite small (Table 2), more similar to that on air-mass or small cloud days, while the TCCL and PW were similar in value to those found on the cold-front days. The PIA sounding on 19 May indicated very strong shear, while shear was weak on 19 July, as on the air-mass days. Late in the afternoon on 19 May, when the vertical shear was strong, CAPE was small, and thus the Ri was small, a "mini-tornado" was observed in the central Illinois area (Kennedy et al., 1989).

### 3.3. Small cloud experimental units

To confirm that the small cloud experimental units were substantially different from the large cloud experimental units, as suggested by earlier midwestern studies and the subjective forecasts made during PACE 1989, the small cloud units also were examined (Table 4). Of the first echo heights of the relatively isolated cores, 86% formed completely below the zero-degree isotherm, similar to those for the air-mass storms. Coalescence likely was an important factor in precipitation formation on these days. The maximum echo tops reached were considerably lower on the small cloud days as well. Values of PB, CAPE, and LI indicated substantially less energy was available for cloud growth, both in the mid- and upper troposphere during these units. These environmental buoyancy estimates appear to be most related to the echo-top height. The PB versus TCCL relationship objectively forecasted a < 60% chance of tall clouds forming on small cloud days.

Thus, the thermodynamic environment, and not simply the type of forcing, was important in determining whether large or small clouds formed. None of the six small cloud units in 1989 were of the air-mass variety. The amount of rainfall produced within the small cloud experimental units in general was less than that found for both the cold-front and air-mass units. The rainfall over the extended network for the same time period was comparable to that of air-mass storms (Table 5).

## 4. COMPARISON OF COLD-FRONT AND AIR-MASS ECHO-CORE PROPERTIES

Nearly equal samples of cold-front and air-mass echo cores were treated in large cloud units, as shown in Table 7. Either sand or AgI treatments were applied to 33 cold-front echo cores and to 27 air-mass cores. The four no-echo clouds were treated during the cold-front units. All air-mass clouds that were treated, echoed. Seven echoes from the other two large cloud units were treated with sand and are not considered here.

### 4.1. Cores at first echo

First echo information from the large sample of echoes within and near the experimental units before, during, and after treatment (Table 6) indicated that cold-front first echoes occurring on days with hail were taller (FEHtp10), colder (FETtp10), and slightly deeper (FEdpth10) than the air-mass echoes. These results are consistent with earlier findings for days with more organized convection and hail (Towery and Changnon, 1970; Changnon and Morgan, 1976; Changnon, 1978b). The cold-front and air-mass first echoes were characterized by similar areas (FEA10) and peak reflectivities (FEMxZ), at the time of first detection. The mean height of the freezing level was similar for the cold front and the air-mass units.

The first echo information for the individually tracked and treated cores (Table 7) likewise indicated that the cold-front cores were taller and colder than the air-mass cores. On cold-front days, 70 to 75% of the treated echo cores were isolated or loosely joined at the time of first echo. In contrast, 70 to 75% of the treated air-mass echo cores were strongly merged at the time of first echo. This could suggest that stronger updrafts occurred on the cold-front days resulting in stronger outflows that initiated new core growth farther from the parent cores, or perhaps that compensating subsidence damped convection for a wider range around the stronger storms, or possibly that gravity waves were interacting with the boundary layer and cloud field on the stronger shear days. Although the air-mass cores were more strongly merged at first-echo, they were tracked on average, 10 minutes longer than the cold-front cores, some 16 minutes beyond the time of their maximum area.

The 27 air-mass first echoes were much more reflective then their cold-front counterparts (Table 7). The initial peak reflectivity was probably greater for the small sample of treated air-mass cores than for the large sample of isolated air-mass cores (Table 6) and the cold-front cores because they were already part of larger systems. Also, because the air-mass cores were joined with the more mature parent systems, their boundaries were somewhat indistinct, perhaps leading to larger values of area and reflectivity. However, the reflectivities might be expected to be greater since the sample of treated air-mass cores were taller and larger than the sample of isolated air-mass cores.

Table 6. First echo (FE) height, temperature, and area, depth, and maximum reflectivity characteristics for the "large" cloud units, stratified by synoptic type from the large sample of isolated FE occurring before and after treatment, within and nearby the experimental units. Student t-test probabilities (P1) and Wilcoxon Rank Sum Test probabilities (P2) for differences in the cold front and air mass cores are presented. The Other category refers to the Squall Zone and Low Pressure experimental units. Variable definitions are found in the Appendix.

| | *Cold Front* | | *Air Mass* | | | | *Other* | |
|---|---|---|---|---|---|---|---|---|
| *Sample* | 160 | | 71 | | | | 23 | |
| | *Mean* | *Std D* | *Mean* | *Std D* | *P1* | *P2* | *Mean* | *Std D* |
| FEHtp10 | 5.3 | 1.5 | 3.7 | 1.0 | <.001 | <.001 | 4.0 | 1.0 |
| FEHMxZ | 4.2 | 1.6 | 2.7 | 1.0 | <.001 | <.001 | 2.7 | 1.6 |
| FEHbs10 | 3.0 | 1.6 | 1.8 | 0.8 | <.001 | <.001 | 1.6 | 0.9 |
| FEtpTmp | -6.5 | 9.1 | 4.7 | 6.2 | <.001 | <.001 | -2.1 | 4.6 |
| FEmzTmp | 0.05 | 9.7 | 9.8 | 6.2 | <.001 | <.001 | 5.0 | 6.0 |
| FEbsTmp | 7.6 | 10.1 | 15.4 | 5.5 | <.001 | <.001 | 10.8 | 5.0 |
| FEA10 | 4.5 | 3.0 | 4.0 | 2.7 | .227 | .232 | 5.7 | 3.2 |
| FEdpth10 | 2.3 | 1.4 | 1.9 | 1.1 | .018 | .018 | 2.3 | 1.2 |
| FEMxZ | 17.9 | 5.7 | 16.6 | 1.9 | .105 | .138 | 17.9 | 5.6 |

Table 7. As in Table 6, but for the samples of treated cores.

| | *Cold Front* | | *Air Mass* | | | | *Other* | |
|---|---|---|---|---|---|---|---|---|
| *Sample* | 33 | | 27 | | | | 7 | |
| | *Mean* | *Std D* | *Mean* | *Std D* | *P1* | *P2* | *Mean* | *Std D* |
| FEHtp10 | 6.6 | 1.5 | 5.7 | 1.4 | .018 | .013 | 5.7 | 1.1 |
| FEHMxZ | 5.4 | 1.7 | 4.2 | 1.4 | .005 | .007 | 4.3 | 1.1 |
| FEtpTmp | -15.0 | 10.3 | -7.6 | 8.9 | .005 | .001 | -12.3 | 8.4 |
| FEmzTmp | -7.2 | 10.6 | 1.1 | 8.6 | .002 | .004 | -4.5 | 6.2 |
| FEA10 | 8.1 | 8.7 | 8.7 | 6.4 | .759 | .414 | 15.4 | 12.0 |
| FEdpth10 | 2.5 | 1.6 | 2.0 | 1.5 | .233 | .256 | 2.1 | 1.1 |
| FEMxZ | 23.2 | 10.6 | 31.0 | 12.5 | .011 | .020 | 28.8 | 6.2 |

4.2. Cores at treatment

Several variables, either radar derived or observed by the seeding aircraft at the time of treatment, have been employed as indicators of subsequent cloud growth (Appendix). These variables were examined to identify any distinction between the cold-front cores and the air-mass cores at the time of treatment.

The mean values of the cold-front cores selected for treatment reveal that they were younger (FECPt), shorter in height (CPHtp10), and smaller in diameter (CPmndia) at the time of treatment (Fig. 1, 2). They also tended to have smaller peak reflectivities (CPMxZ) and contain smaller amounts of liquid water (LWCd) as measured by two-dimensional (2D)-P and 2D-C probes (Table 8). The smaller peak reflectivity and size may be due in part to the fact that the cold-front cores were younger at the time of treatment. The aircraft measurements confirmed that the cold-front clouds had smaller fractions of the total condensate in the solid phase (SWC_frac) at the time of treatment, which would be expected in younger clouds. Likewise, the change in height (CPFEdH10), area (CPFEdA10), and reflectivity (CPFEdZ) from first echo to treatment should be greater for the older air-mass cores (Table 8). These differences are statistically significant, using both the Student's t-test and the Wilcoxon Sum Rank test.

The horizontal growth rates of the cores (CPFEdAdt) were estimated from the time of first echo to the time of treatment (Fig. 2), and indicated that the air-mass cores were growing more rapidly in area than the cold-front cores. Aircraft measurements of mean net buoyancy (NBuoy) indicated that the cold-front clouds were more negatively buoyant. Estimated vertical growth at the time of treatment (V_cdp), derived from the rate of change of the 10-dBZ reflectivity contour defining the height of the echo top, indicated that most echoes were growing slowly at the time of treatment, although a few were growing very rapidly. Ten cold-front cores indicated negative vertical growth, as compared to only three air-mass cores.

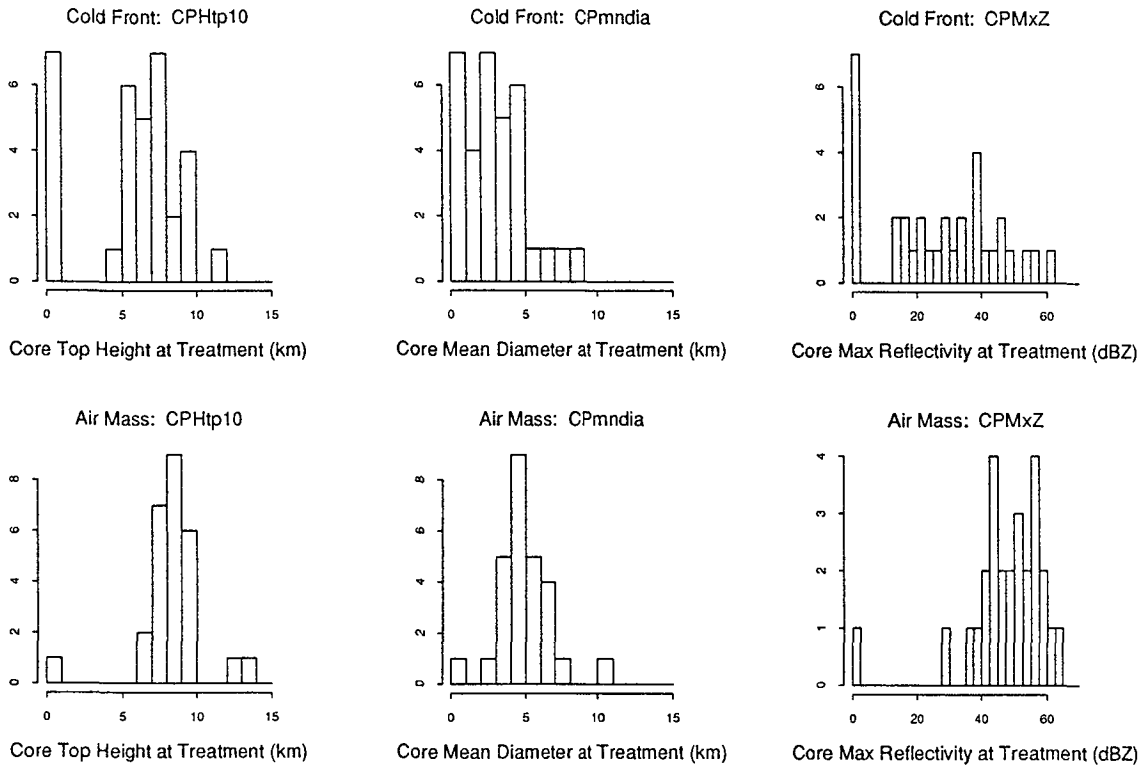


*Figure 1. Frequency histograms of echo-core top height, mean diameter, and peak reflectivity at the time of treatment, according to synoptic weather condition.*

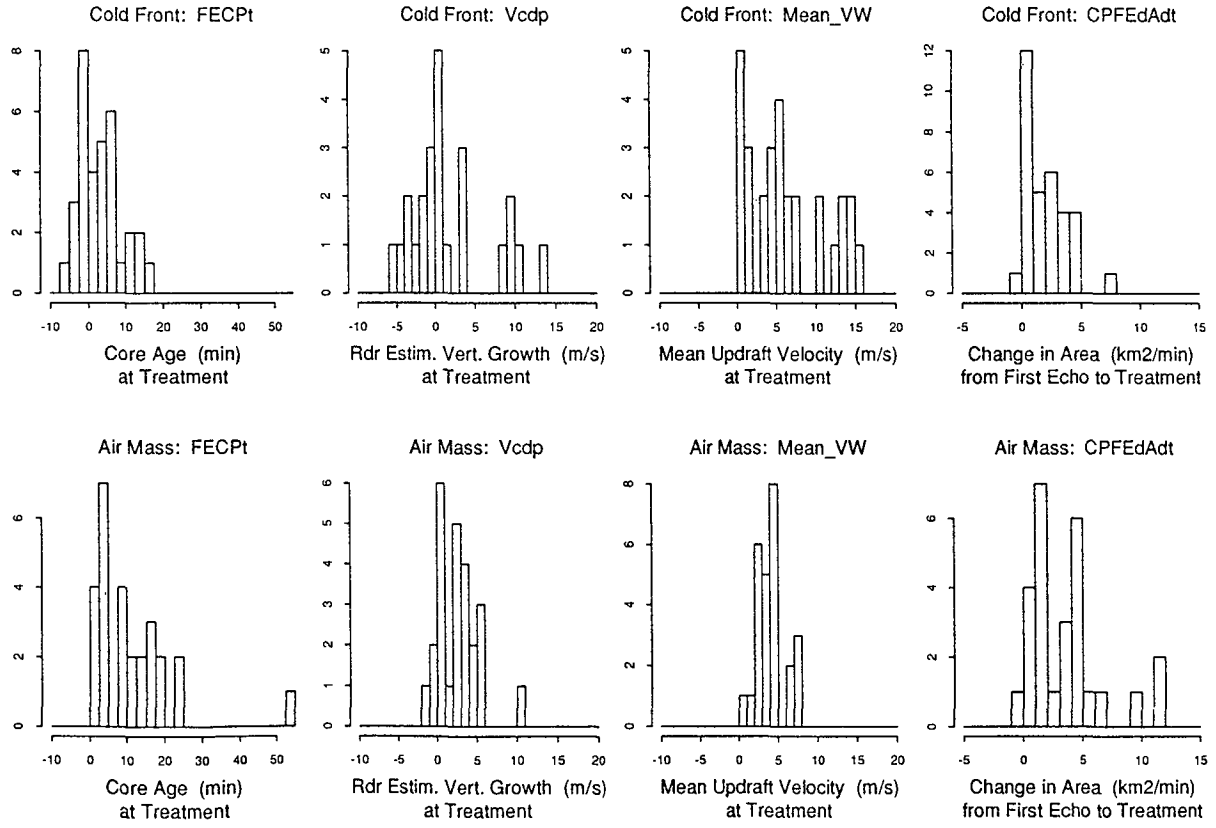


*Figure 2. Frequency histograms of echo-core age, radar-estimated vertical motion and mean updraft speed at the time of treatment, and the rate of change in horizontal area between the time of first echo and treatment, according to synoptic weather condition.*

Table 8. Predictor variables at the time of treatment for echo cores under cold front (CF) and air mass (AM) conditions. P1 and P2 are probabilities that the samples are the same, using the Student's t-test and the Wilcoxon Rank Sum test, respectively.

| *Predictor* | *Mean* | | *Std. Dev.* | | *P1* | *P2* | *Sample* | |
|---|---|---|---|---|---|---|---|---|
| *Variable* | *CF* | *AM* | *CF* | *AM* | | | *CF* | *AM* |
| CPmndia | 2.9 | 4.9 | 2.2 | 2.0 | <.001 | <.001 | 33 | 27 |
| CPHtp10 | 5.4 | 7.9 | 3.2 | 2.2 | .001 | <.001 | 33 | 27 |
| CPMxZ | 26.8 | 47.5 | 18.6 | 12.6 | <.001 | <.001 | 33 | 27 |
| FECPt | 3.3 | 11.2 | 5.6 | 10.9 | .001 | <.001 | 33 | 27 |
| Mean_VW | 6.2 | 3.9 | 4.9 | 1.8 | .033 | .121 | 29 | 26 |
| UP_dia | 1.4 | 1.3 | 1.0 | 0.8 | .634 | .859 | 29 | 26 |
| SWC_frac | .056 | .306 | .120 | .350 | .002 | .029 | 24 | 25 |
| LWCd | .168 | .264 | .448 | .535 | .504 | .003 | 24 | 25 |
| NBuoy | -1.38 | -0.44 | 1.81 | 1.60 | .059 | .043 | 24 | 25 |
| Buoy-Enh | 0.49 | 0.51 | 0.08 | 0.03 | .121 | .219 | 24 | 25 |
| CPFEdH10 | 0.2 | 2.2 | 1.4 | 2.6 | <.001 | <.001 | 33 | 27 |
| CPFEdA10 | 10.8 | 28.6 | 15.3 | 30.7 | .005 | .002 | 33 | 27 |
| CPFEdZ | 10.4 | 16.4 | 10.9 | 15.6 | .086 | .117 | 33 | 27 |
| Vcdp | 1.7 | 2.5 | 5.1 | 2.5 | .456 | .002 | 24 | 25 |
| CPFEdAdt | 1.97 | 3.55 | 1.90 | 3.21 | .021 | .029 | 33 | 27 |
| CPFEdZdt | 2.41 | 1.98 | 2.87 | 2.30 | .532 | .911 | 33 | 27 |

Updraft velocity (Mean_VW) was estimated using aircraft measurements (Fig. 2). While most updrafts ranged from 0 to 7 $ms^{-1}$ on cold-front days, they exceeded 10 $ms^{-1}$ in about 25% of the cores. Updrafts ranged from 0 to 7 $ms^{-1}$ in the air-mass clouds. The mean speed was larger for the cold-front clouds. This difference was statistically significant at the 5% level according to the Student's t-test (Table 8).

The radar-estimated vertical growth and mean updraft speed were best correlated for cores with lower updraft speeds, which occurred on air-mass days. The mean vertical growth was lower than the mean updraft velocity and the largest differences were found for updraft speeds greater than 10 $ms^{-1}$. The lower mean radar-derived vertical motions may have resulted from several factors: 1) The echoes formed at relatively high levels on cold-front days, with only 12% growing more than 1 km prior to treatment. On air-mass days, however, the first echoes formed on average 1 km lower, so a growth measurement could be made from a lower starting elevation on those days. About 70% of the air-mass cores had grown more than 2 km by treatment time, and 33% had grown more than 3 km. Thus prior to treatment the air-mass cores overall started lower and grew taller than the cold-front cores, allowing a better growth estimate. 2) The lower echo growth values on cold-front days could also have been caused in part by assigning a value of zero to the updraft speed of the few clouds where no updraft was observed, while the radar estimate of vertical growth included some negative values.

The air-mass cores were larger at the time of treatment, and the radar-based estimates of horizontal and vertical growth indicated that they were growing more in height and area than the cold-front cores. This was corroborated by greater negative values of net buoyancy for the cold-front cores.

### 4.3. Core maximum values

Echo behavior characteristics after treatment were defined as response variables (Fig. 3, 4, Table 9). Between the cold-front and the air-mass cores, the latter were taller (MaxH10), larger in area (MaxA10), more reflective (MaxZ), and longer lasting (FECPtMxA). However, only the differences in maximum reflectivity and the change in maximum reflectivity (MXCPdZ) were statistically different by both the Wilcoxon and t-tests. The reflectivity of the cold-front cores may have changed greatly after treatment because they were younger at the time of treatment. In the mean, the cold-front cores were 3.3 min old at treatment, with a peak reflectivity of 26.8 dBZ. The air-mass cores, however, were 11.2 minutes old at treatment with a mean peak reflectivity of 47.5 dBZ. However, the air-mass cores attained higher maximum

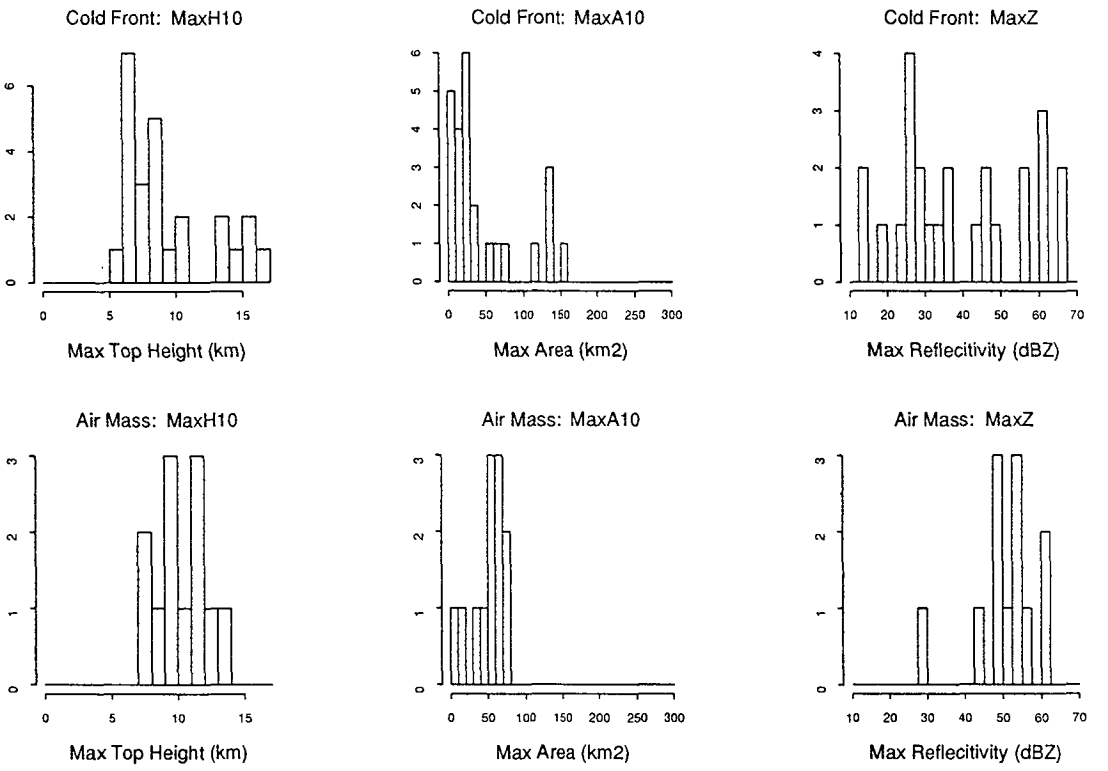


*Figure 3. Frequency histograms of maximum echo-core height, area, and reflectivity, according to synoptic weather condition.*

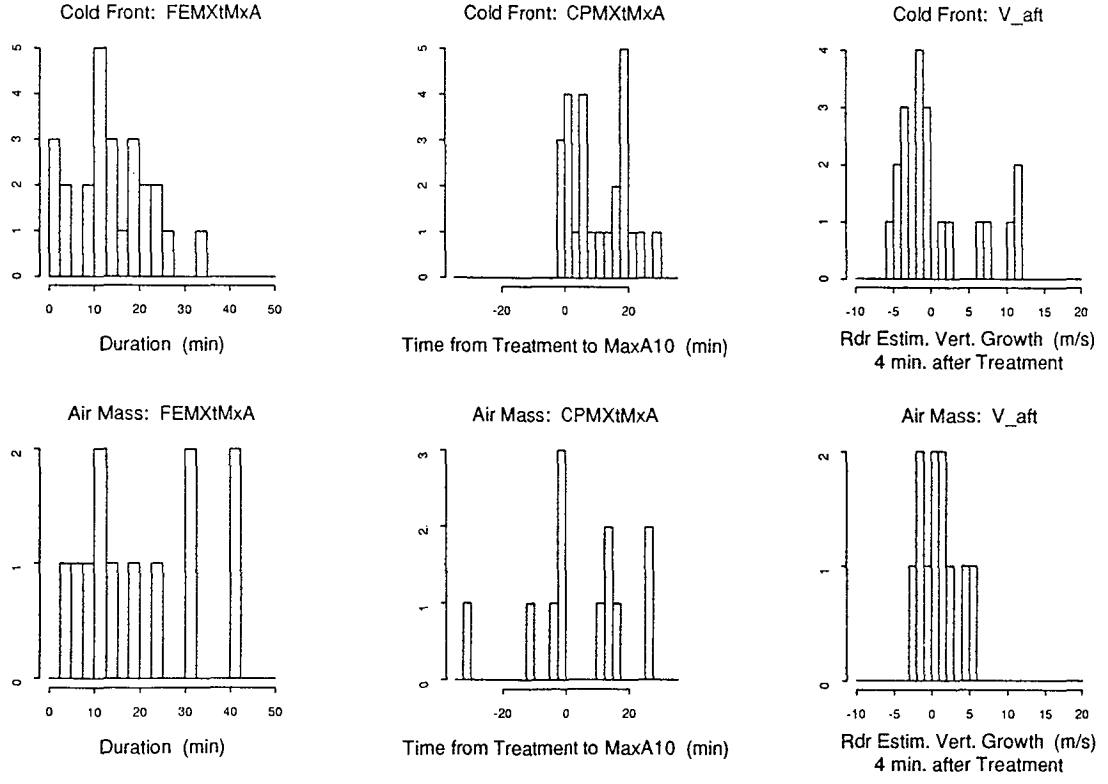


*Figure 4. Frequency histograms of echo-core duration, duration following treatment, and radar-estimated vertical motion 4 minutes after treatment, according to synoptic weather condition.*

Table 9. Response variables for echo cores under cold front (CF) and air mass (AM) conditions. P1 and P2 are probabilities that the samples are the same, using the Student's t-test and the Wilcoxon Rank Sum test, respectively.

| *Response* | *Mean* | | *Std. dev.* | | *P1* | *P2* | *Sample* | |
|---|---|---|---|---|---|---|---|---|
| *variable* | *CF* | *AM* | *CF* | *AM* | | | *CF* | *AM* |
| MaxH10 | 8.8 | 9.5 | 3.2 | 1.7 | .355 | .080 | 33 | 27 |
| MaxA10 | 46.7 | 72.0 | 45.0 | 58.3 | .063 | .015 | 33 | 27 |
| MaxZ | 41.6 | 54.4 | 15.4 | 8.1 | <.001 | .001 | 33 | 27 |
| MXCPdH10 | 1.2 | 1.0 | 2.9 | 2.2 | .750 | .349 | 33 | 27 |
| MXCPdA10 | 28.3 | 26.3 | 40.5 | 49.0 | .862 | .988 | 33 | 27 |
| MXCPdZ | 12.6 | -0.2 | 16.5 | 10.3 | .001 | .002 | 33 | 27 |
| CPMXtMxA | 10.1 | 6.3 | 8.5 | 12.5 | .164 | .196 | 33 | 27 |
| FEMXtMxA | 13.4 | 17.5 | 7.7 | 11.6 | .111 | .319 | 33 | 27 |
| Vaft | 1.7 | 1.3 | 5.7 | 1.9 | .737 | .285 | 28 | 25 |
| MXCPdAdt | 1.54 | 1.51 | 2.86 | 5.71 | .982 | .761 | 33 | 27 |
| MXCPdZdt | 1.48 | 2.09 | 0.77 | 1.30 | .027 | .086 | 33 | 27 |

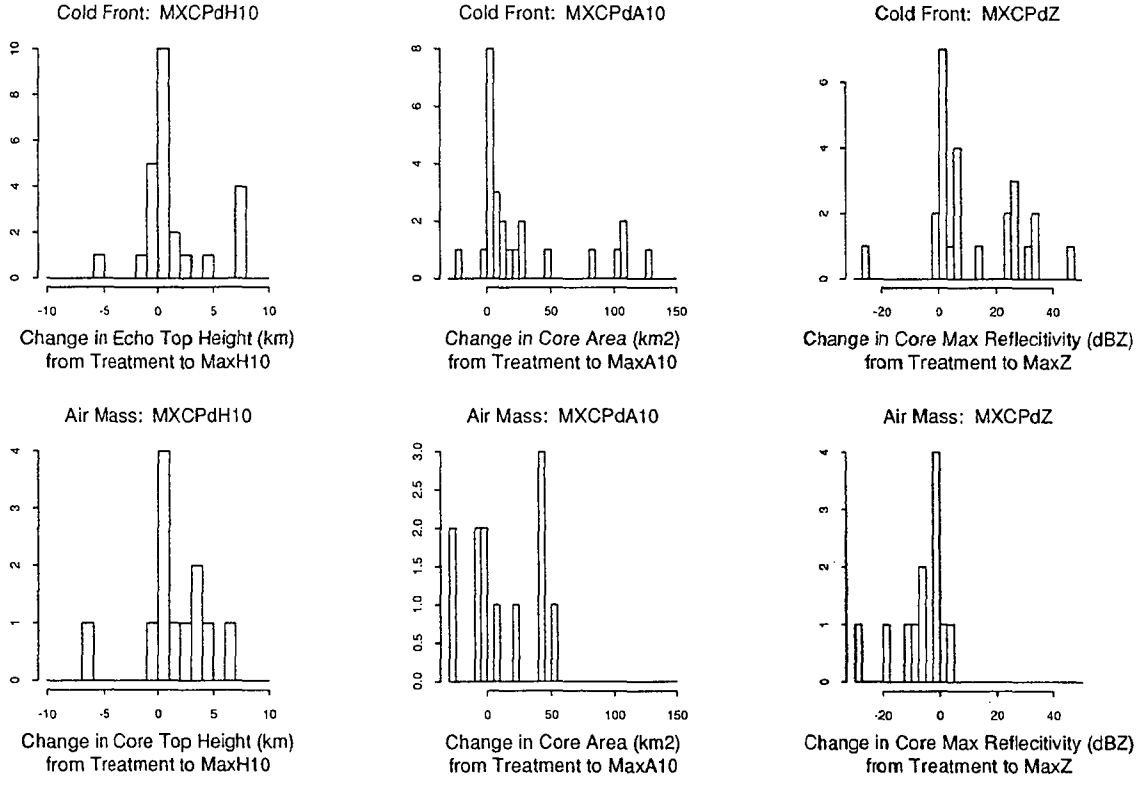


*Figure 5. Frequency histograms of the change in height, horizontal area, and peak reflectivity following treatment, according to synoptic weather condition.*

reflectivities. Maximum reflectivity values achieved for cold-front and air-mass cores were 41.6 and 54.4 dBZ, respectively.

Both types of cores experienced similar mean changes and rates of change in height (MXCPdH10, V_aft) and area (MXCPdA10, MXCPdAdt) after treatment, although the maximum values were again larger for the air-mass cores (Fig. 5). Overall, the cold-front cores grew less and ended sooner, either through dissipation or merger. In fact, not even half (42%) of the cold-front cores grew in height at all during their history. On the other hand, 85% of the air-mass cores grew more than 2 km, and 74% grew more than 3 km in height during their life span. Thus, the differences in maximum values seem to be related to the echoes' behavior before and at the time of treatment.

### 4.4. Cold-front versus air-mass echo-core properties

The cold-front experimental units had the tallest daily echo tops and some of the tallest, largest, and most reflective echo cores, and the strongest updrafts. Hail was produced on these days, there was a large amount of potential buoyancy present in the atmosphere, and vertical shear was stronger than on air-mass days. In addition, past studies have shown that cold-front storms are longer lasting and generally produce more rain than air-mass storms (Changnon, 1980; Vogel, 1977). This was largely the case for the 1989 storms: more mean rainfall was produced during cold-front periods within the experimental unit and for a 240 x 240-km area around CMI (Table 10). In fact, three of the five cold-front experimental units produced more than 200 x $10^4$ $m^3$ of rain from 15 minutes before treatment to 15 minutes after treatment (Table 3). Only one of the four air-mass cores produced comparable rain. The four largest rain-producing systems, whether cold-front or air-mass storms, were lines (Table 3).

Thus, in the mean, the cold-front cores could be expected to be larger than the air-mass cores. Instead, a broad, perhaps bi-modal distribution was present in vertical motion parameters at the time of treatment; in maximum height, area, and reflectivity, in the change in core area and reflectivity after treatment; and in the estimate of vertical growth 4 minutes after treatment. Of the cold-front cores that were approachable for treatment, there were many small cores and a few large ones. On average, the air-mass cores were larger, longer lasting, and more reflective.

The smaller cold-front cores may be explained in part by the results of Newton and Newton (1959). The stronger vertical shear on cold-front days may inhibit the growth of the smaller cores, as the rapid entrainment of stronger horizontal winds into a narrow cloud results in a cloud more prone to dissipate. The growth of the wider cores (Fig. 3, 9) with stronger updrafts is likely enhanced by the kinetic energy drawn from the wind field under strong shear conditions. The cores with the largest areas were found on the higher shear days as suggested by the results of Lemone (1989). However, the air-mass cores were generally larger, taller, and more often merged with another air-mass core at the time of treatment. In this more protected environment, less affected by vertical shear, even the small cold-front cores grew.

## 5. EVALUATION FOR POTENTIAL SEEDING EFFECTS

### 5.1. Cold-front cores

During the six cold-front experimental units, 21 cores were treated with AgI and 12 with sand flares. P-values indicating the level of significance of differences in the AgI and sand populations were computed in two ways: First, the P-values were computed assuming that the echo cores even within

Table 10. Fifteen minute rainfall accumulations for the 1989 Illinois experimental units and for the extended network area, a 240 x 240 km area centered on CMI. BT refers to the Beginning of Treatment and ET to the End of Treatment. The treatment periods ranged from 10 to 48 min. and have been normalized to a 15 min. period.

| | Experimental Unit | | Extended Network | |
|---|---|---|---|---|
| Time in Minutes | Cld Frnt, n=5 ($10^4$ $m^3$) | Air Mass, n=4 ($10^4$ $m^3$) | Cld Frnt, n=5 ($10^6$ $m^3$) | Air Mass, n=4 ($10^6$ $m^3$) |
| | Mean (StdD) | Mean (StdD) | Mean (StdD) | Mean (StdD) |
| BT - 15 | 34.1 (27.7) | 23.6 (14.9) | 11.8 ( 6.7) | 4.2 ( 1.7) |
| BT - ET | 64.6 (58.5) | 24.4 (20.6) | 14.5 ( 8.7) | 4.4 ( 2.6) |
| ET + 15 | 110.2 (91.6) | 20.5 (23.3) | 19.1 (12.4) | 2.5 ( 3.0) |
| +15 to +30 | 117.3 (107.4) | 16.1 (17.8) | 19.6 (12.7) | 1.6 ( 0.9) |
| +30 to +45 | 78.8 (61.3) | 15.5 (14.0) | 18.1 (10.6) | 2.1 ( 2.0) |
| +45 to +60 | 70.4 (68.8) | 9.9 (11.3) | 16.9 (11.5) | 1.5 ( 1.4) |
| +60 to +75 | 94.2 (124.6) | 7.4 ( 8.1) | 20.9 (13.6) | 1.4 ( 1.3) |
| +75 to +90 | 108.6 (138.5) | 20.7 (37.7) | 20.8 (19.2) | 3.3 ( 4.3) |

the experimental units were independent entities. Secondly, the P-values were computed using a rerandomization scheme which grouped the cores by experimental units. The combinations of Agl and sand units were determined using the same rules intended in the actual experiment: that no consecutive units in a single flight could receive the same treatment, and that no more than two consecutive units could receive the same treatment. This resulted in 208 unique combinations for the 12 experimental units (Czys et al., 1993). The sub-sample of cold-front units resulted in 20 unique combinations, resulting in a minimum attainable P-value of about .05.

At the time of first echo, the Agl-treated cores were smaller in horizontal area and shorter than the sand-treated cores (Table 11). Significant differences, however, were only observed when the cores were treated as statistically independent entities.

At the time of treatment, the sand-treated cores were generally younger than the Agl-treated cores. The mean height, area, reflectivity, and fraction of solid water content of the Agl- and sand-treated cores were nearly the same. However, both the radar and the aircraft estimated vertical growth was greater for the sand- than the Agl-treated cores. Larger changes and rates of change in height, area, and reflectivity between first echo and treatment also were noted for the younger sand-treated cores. Thus, even though the mean height, area, and reflectivity were similar at treatment for the Agl- and sand-treated cores, the sand-treated cores appeared to be growing more vigorously at that time. By treatment time, 11 clouds had not echoed. Four of the seven Agl-treated clouds never echoed, the four sand-treated cores did eventually echo.

Table 11. Predictor variables at the time of treatment for echo cores under cold-front conditions. T is the probability that the sample means are the same, using the Student's t-test. TR is the probability based on a rerandomization of the experimental units.

| | Mean | | Std. Dev. | | | | Sample | |
|---|---|---|---|---|---|---|---|---|
| Predictor Variable | Agl | Sand | Agl | Sand | T | TR | Agl | Sand |
| FEHtp10 | 6.2 | 7.3 | 1.3 | 1.8 | .069 | .279 | 21 | 12 |
| FEHMxZ | 5.0 | 6.0 | 1.5 | 1.8 | .099 | .279 | 21 | 12 |
| FEA10 | 5.7 | 12.3 | 3.9 | 12.7 | .033 | .240 | 21 | 12 |
| FEmxZ | 22.3 | 24.9 | 9.5 | 12.6 | .578 | .519 | 21 | 12 |
| CPmndia | 2.8 | 3.1 | 1.7 | 2.9 | .665 | .298 | 21 | 12 |
| CPHtp10 | 5.3 | 5.4 | 2.6 | 4.2 | .911 | .901 | 21 | 12 |
| CPMxZ | 26.9 | 26.6 | 16.2 | 23.0 | .972 | 1.00 | 21 | 12 |
| FECPt | 4.3 | 1.5 | 5.4 | 5.7 | .160 | .279 | 21 | 12 |
| Mean_VW | 4.4 | 8.8 | 4.5 | 4.5 | .016 | .519 | 17 | 12 |
| UP_dia | 1.1 | 1.9 | 1.1 | 0.8 | .031 | .375 | 17 | 12 |
| SWC-frac | .085 | .027 | .152 | .070 | .239 | .760 | 12 | 12 |
| LWCd | .201 | .136 | .518 | .387 | .732 | .625 | 12 | 12 |
| NBuoy | -1.38 | -1.38 | 1.77 | 1.92 | .993 | 1.00 | 12 | 12 |
| Buoy-Enh | 0.45 | 0.52 | 0.08 | 0.06 | .020 | .144 | 12 | 12 |
| CPFEdH10 | -0.2 | 0.8 | 1.5 | 1.0 | .037 | .144 | 21 | 12 |
| CPFEdA10 | 9.1 | 13.7 | 13.3 | 18.4 | .421 | .279 | 21 | 12 |
| CPFEdZ | 7.7 | 15.3 | 8.8 | 12.9 | .053 | .048 | 21 | 12 |
| Vcdp | -0.2 | 4.3 | 3.6 | 5.8 | .027 | .346 | 14 | 10 |
| CPFEdAdt | 1.27 | 3.21 | 1.33 | 2.17 | .003 | .048 | 21 | 12 |
| CPFEdZdt | 1.55 | 3.91 | 2.50 | 2.96 | .021 | .048 | 21 | 12 |

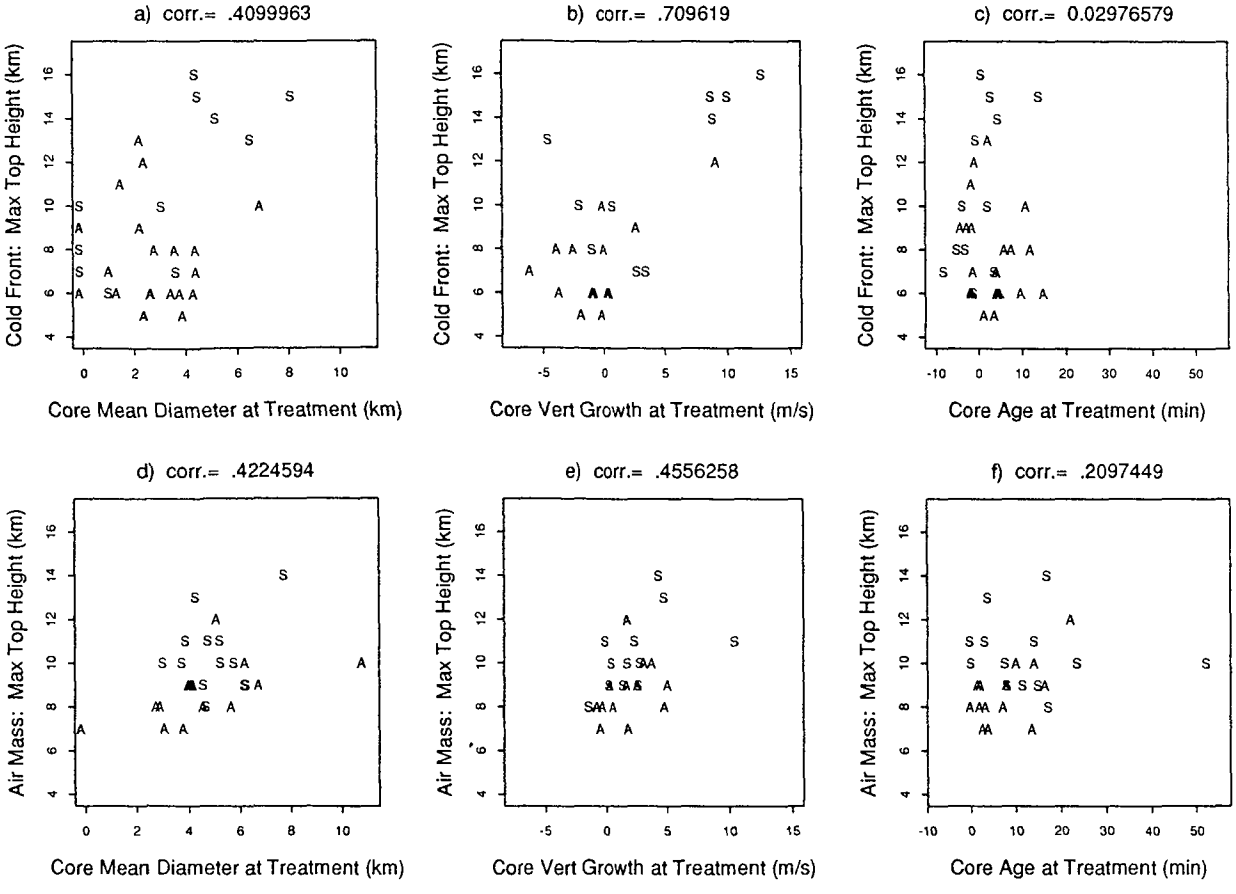


*Figure 6. Scatter plots of echo-core mean diameter, radar-estimated vertical growth, and age at treatment versus the maximum height attained by the cores. The A and S refer to AgI- and sand-treated cores, respectively. The data are stratified by synoptic weather condition. The a to c refer to cold-front cores, and d to f refer to air-mass cores.*

For cloud seeding operations, these findings suggest that when the atmosphere is characterized by moderate to strong vertical shear and large values of potential buoyancy, the sample of clouds that are approachable by a seeding aircraft may be characterized by many small and a few large clouds, with the large clouds growing regardless of treatment. From these data it is not at all apparent that AgI treatment assisted in the growth on either the small or the larger echo cores. On cold-front days, it may be more difficult to find a positive seeding effect on a cloud by cloud basis, even without a sampling bias.

5.2. Air-mass cores

During the four air-mass experimental units, 14 cores were treated with AgI and 13 with sand. As there were only four air-mass units, only six unique rerandomization permutations were possible. Because of this, the minimum P-value using the rerandomization scheme was about .17.

At the time of first echo and at treatment, the air-mass AgI-treated and sand-treated cores were generally alike (Table 13). The bias at treatment time appears to be confined to the cold-front cores. However, the sand-treated cores grew taller than the AgI-treated cores and demonstrated a greater mean change in height after treatment (Table 14). Since cloud seeding was expected to increase vertical growth, if a seeding effect was present, it acted in a negative way. However, these values were only significant considering the cores as independent entities. Additionally, in terms of maximum horizontal area and reflectivity no seeding effect was suggested as the sand- and AgI-treated cores were similar in mean value. Because only height was different for the AgI and sand cores, it is not clear that AgI treatment was the cause of the lower maximum heights.

It is possible that different covariates measured at the time of first echo or at treatment may better predict the maximum values expected for echo cores on these days. No relationship was found between core diameter (Fig. 6d) or vertical growth (Fig. 6e) at treatment and the maximum echo top attained for the air-mass cores treated with either AgI or sand (Fig. 6f). The sand-treated cores were generally taller for any given age group, for any given range of core diameter (Fig. 6d), and for any given range of updraft velocity (Fig. 6e).

For this small group of echo cores, AgI-treatment did not invigorate the treated cores during their early history. Thus, these results do not confirm the early steps of the dynamic seeding hypothesis.

From the dynamic seeding hypothesis, it was expected that the AgI-treated cores would grow more after treatment and taller overall than the sand-treated cores. The sand-treated cores, however, attained greater heights than did the AgI-treated cores, although these values were only significant considering the cores as independent entities (Table 12). The sand-treated cores also had significantly longer growth periods, from first echo to maximum areal extent. Following treatment, a longer period of time to reach the maximum area was found for the sand cores, but this might in part be due to the younger age of the sand-cores at treatment. In the mean, the sand-treated cores grew more before treatment and continued to grow more after treatment in terms of height, area, and reflectivity. That is, the cores treated with sand were more vigorous before and after treatment.

The tallest cold-front echoes, whether treated with sand or AgI exhibited the largest radar-estimated vertical growth at treatment, and stronger and wider updrafts near cloud top. Five of the tallest echo cores had a mean core diameter >4 km at treatment, and were treated with sand. Aircraft measurements of updraft speed indicated that eight of the cold-front cores had updrafts >9 $ms^{-1}$, and six of these eight cores reached heights of more than 10 km. The other two cores had mean updraft diameters of <1.5 km. In addition, two cores with weaker updraft speeds, but with updraft diameters >1.5 km, reached more than 10 km. Updraft diameter (.73) was better correlated than core diameter (.41) with maximum height. None of the cold-front cores with updraft diameters <1.5 km grew more than 10 km in height. Whereas, three cores with diameters <3 km, grew to greater than 10 km.

Of the 18 cold-front cores with diameters of less than 5 km that were echoing at treatment, 13 were treated with AgI. This bias towards smaller diameters at treatment for the AgI-treated cores renders it impossible to determine if a seeding effect is present.

Rosenfeld and Woodley (1989) in Texas and Gagin et al. (1986) in Florida examined a group of echo cores (short-track cells) that are similar to the 1989 Illinois echo cores (Changnon et al., 1993). In both Texas and Florida the short-tracked cells that were young at the time of treatment and that were treated with many flares responded in a positive way to seeding in terms of duration and areal extent. In Texas, no difference was found in maximum height for that particular sample of cores, nor for the sample as a whole. In Florida, the young, heavily AgI-treated cores, making up about 15% of the whole sample, grew taller. For the Florida sample as a whole, no difference was found in the maximum height attained by the individual cores.

In Illinois, only two cores were treated early, with more than 8 flares. Comparing AgI and sand-treated core differences in height, the cores treated early with more than 6 flares, and the remaining population reacted similarly. Little or no correlation was found between core age alone at treatment and the maximum height of the echo core (Fig. 6). Most cold-front cores were treated within 5 minutes of first echo. The three tallest AgI-treated cores were treated within 5 minutes of first echo. However, eight others also treated with AgI within 5 minutes of first echo did not reach 10 km in height. It appears that for the cold-front cores, the size of the core at treatment and its vertical growth is more important than its age.

Table 12. Response variables for echo cores under cold-front conditions. T is the probability that the sample means are the same using the Student's t-test. TR is the probability based on a rerandomization of the experimental units.

| Response | Mean | | Std. Dev. | | | | Sample | |
|---|---|---|---|---|---|---|---|---|
| Variable | AgI | Sand | AgI | Sand | T | TR | AgI | Sand |
| MaxH10 | 7.8 | 10.8 | 2.3 | 3.6 | .007 | .125 | 21 | 12 |
| MaxA10 | 36.9 | 63.9 | 35.3 | 55.9 | .098 | .279 | 21 | 12 |
| MaxZ | 40.2 | 44.2 | 13.2 | 19.0 | .479 | .625 | 21 | 12 |
| MXCPdH10 | 0.4 | 2.6 | 2.4 | 3.3 | .036 | .375 | 21 | 12 |
| MXCPdA10 | 19.8 | 43.3 | 36.8 | 43.3 | .108 | .279 | 21 | 12 |
| MXCPdZ | 9.7 | 17.5 | 17.8 | 13.1 | .195 | .433 | 21 | 12 |
| CPMXtMxA | 7.2 | 15.3 | 7.5 | 8.0 | .006 | .125 | 21 | 12 |
| FEMXtMxA | 11.5 | 16.8 | 5.7 | 9.8 | .058 | .048 | 21 | 12 |
| Vaft | .71 | 3.56 | 5.85 | 5.14 | .210 | .750 | 18 | 10 |
| MXCPdAdt | 1.12 | 2.28 | 3.24 | 1.94 | .419 | .279 | 21 | 12 |
| MXCPdZdt | 1.60 | 1.26 | 0.77 | 0.75 | .234 | .510 | 21 | 12 |

Table 13. Predictor variables for echo cores under air-mass conditions.

| Predictor | Mean | | Std. Dev. | | | | Sample | |
|---|---|---|---|---|---|---|---|---|
| Variable | Agl | Sand | Agl | Sand | T | TR | Agl | Sand |
| FEHtp10 | 5.6 | 5.7 | 1.3 | 1.6 | .930 | 1.00 | 14 | 13 |
| FEHMxZ | 4.5 | 3.8 | 1.5 | 1.2 | .238 | .385 | 14 | 13 |
| FEA10 | 7.1 | 10.5 | 6.6 | 6.0 | .184 | .385 | 14 | 13 |
| FEMxZ | 28.3 | 34.0 | 12.2 | 12.6 | .240 | .615 | 14 | 13 |
| CPmndia | 4.7 | 5.2 | 2.5 | 1.2 | .541 | .385 | 14 | 13 |
| CPHtp10 | 7.4 | 8.3 | 2.6 | 1.6 | .308 | .385 | 14 | 13 |
| CPMxZ | 44.4 | 50.7 | 15.4 | 8.0 | .201 | .385 | 14 | 13 |
| FECPt | 8.5 | 14.1 | 6.7 | 13.8 | .182 | .385 | 14 | 13 |
| Mean_VW | 3.4 | 4.4 | 1.7 | 1.8 | .175 | .385 | 14 | 13 |
| UP_dia | 1.1 | 1.5 | 0.8 | 0.8 | .275 | .769 | 13 | 13 |
| SW_frac | .287 | .323 | .341 | .371 | .807 | 1.00 | 12 | 13 |
| LWCd | .336 | .197 | .728 | .275 | .528 | .615 | 12 | 13 |
| NBuoy | -1.04 | 0.11 | 1.40 | 1.64 | .072 | .385 | 12 | 13 |
| Buoy_Enh | 0.51 | 0.51 | 0.03 | 0.02 | .909 | 1.00 | 12 | 13 |
| CPFEdH10 | 1.8 | 2.6 | 3.0 | 2.1 | .416 | .385 | 14 | 13 |
| CPFEdA10 | 30.4 | 26.7 | 38.6 | 20.4 | .763 | 1.00 | 14 | 13 |
| CPFEdZ | 16.2 | 16.7 | 17.0 | 14.7 | .929 | 1.00 | 14 | 13 |
| Vcdp | 2.2 | 2.8 | 2.0 | 3.1 | .543 | .385 | 13 | 13 |
| CPFEdAdt | 3.74 | 3.35 | 3.50 | 3.00 | .760 | .769 | 14 | 13 |
| CPFEdZdt | 2.40 | 1.52 | 2.60 | 1.93 | .334 | .769 | 14 | 13 |

Table 14. Response variables for echo cores under air-mass conditions.

| Response | Mean | | Std. Dev. | | | | Sample | |
|---|---|---|---|---|---|---|---|---|
| Variable | Agl | Sand | Agl | Sand | T | TR | Agl | Sand |
| MaxH10 | 8.6 | 10.4 | 1.4 | 1.7 | .007 | .385 | 14 | 13 |
| MaxA10 | 68.4 | 75.8 | 53.6 | 65.0 | .748 | .615 | 14 | 13 |
| MaxZ | 54.0 | 54.9 | 9.6 | 6.4 | .794 | 1.00 | 14 | 13 |
| MXCPdH10 | 0.2 | 1.8 | 2.2 | 2.0 | .064 | 1.00 | 14 | 13 |
| MXCPdA10 | 27.4 | 25.2 | 38.4 | 60.0 | .910 | .615 | 14 | 13 |
| MXCPdZ | 1.8 | -2.3 | 13.1 | 5.9 | .303 | 1.00 | 14 | 13 |
| CPMXtMxA | 7.3 | 5.3 | 6.2 | 17.2 | .688 | .615 | 14 | 13 |
| FEMXtMxA | 15.7 | 19.4 | 9.8 | 13.5 | .423 | .769 | 14 | 13 |
| Vaft | 1.3 | 1.4 | 1.5 | 2.4 | .901 | 1.00 | 13 | 12 |
| MXCPdAdt | 2.39 | 0.57 | 6.31 | 5.06 | .419 | .615 | 14 | 13 |
| MXCPdZdt | 2.40 | 1.75 | 1.32 | 1.23 | .196 | .769 | 14 | 13 |

## 6. SUMMARY AND CONCLUSIONS

The 1989 cloud data were partitioned according to synoptic weather conditions. Most rain cases were associated with either cold-front or air-mass conditions. These two conditions had different thermodynamic and kinematic properties, which were reflected in the characteristics of the cores at the time of first echo and at the time of treatment. Due to the small number of cores sampled (33 cold-front and 27 air-mass) and because of the small number of experimental units sampled on these days (6 cold-front, 4 were air-mass), it is not clear how representative these results are for other summers.

The cold-front units had more potential energy available for growth, and somewhat stronger shear than the air-mass units. On the cold-front days, clouds taller than 16 km were present somewhere in the study area, hail was observed, and in general, more rain was produced. However, in the mean, the air-mass cores were larger than the cold-front cores. The cold-front sample contained many small and a few large cores at the time of treatment. The cores that were more vigorous at the time of treatment grew the largest. At the time of first echo and at the time of treatment, the cold-front cores tended to be more separate from their parent core, whereas many air-mass cores were already merged with their parent core. Also, unlike the cold-front cores, all air-mass cores contained echoes at the time of treatment. The smaller cold-front cores might have been more vulnerable to the detrimental effects of entrainment. The largest cold-front cores showed the strongest updrafts sampled and the greatest radar-estimated horizontal and vertical growth.

The cold-front and air-mass units were stratified by treatment type. Of the cold-front clouds, a disproportionate number of small cores were treated with AgI, while the larger cores were treated with sand. Also, before and at the time of treatment, the mean growth rates were larger for the cold-front sand-treated cores. Thus, it was not surprising that the sand-treated cores reached maximum heights greater than the AgI cores. No seeding effect could be deduced from the cold-front sample.

A bias was not evident in the core parameters for the air-mass cores at the time of first echo or at treatment. In examining the maximum values attained by the air-mass cores, the sand-treated cores grew taller than did the AgI-treated cores, although this was only significant considering the cores as independent entities. In terms of core duration, maximum horizontal area, and reflectivity, the sand- and AgI-treated air-mass cores were similar. Thus, the air-mass population showed no other possible seeding response for any parameter other than height.

The data presented here pertain only to the early steps of the dynamic seeding hypothesis. The results do not support the early steps of the dynamic seeding hypothesis which propose that treatment with silver iodide should invigorate a cloud such that it will grow taller.

In partitioning the data by weather conditions, it was found that, particularly in the early growth period of the cold-front and air-mass echo cores, their characteristics differed. It is possible that different covariates measured at the time of first echo or at treatment may better predict the maximum values expected for echo cores on days with differing weather conditions. In particular, the core and updraft diameter at treatment time and the vertical and horizontal growth rates were better correlated with maximum top height on cold-front days than on air-mass days. While the impact of these differing growth behaviors on the way a cloud responds to silver iodide seeding is unclear, inclusion of similar analysis in future seeding experiments is important, at least in Illinois.

This research does not examine later steps of the hypothesis relating to the growth of adjacent or subsequent clouds, nor are other ways in which silver iodide might impact cloud growth addressed. Examination of larger storm scales would have resulted in even smaller samples. As evidenced by differences between rainfall amounts and storm types found on cold-front and air-mass days, and by their variability within cold-front and air-mass categories, the ability to find a significant seeding effect in a single season is not possible. Seeding effects resulting from either the transport of seeding material to other clouds or by cloud interactions would best be addressed on a case study basis or in a multiyear program.

## ACKNOWLEDGMENTS

The authors would like to thank Carl Lonnquist and Julia Chen for their programming expertise, Dr. Ruben Gabriel for his statistical advice, and the two anonymous reviewers for their comments. Much of the computer work was supported by the University of Illinois National Center for Supercomputing. This research was conducted as part of the Illinois component of NOAA's Atmospheric Modification Program under cooperative agreements COM-NA89RAH09086, COM-NA90AA-H-OA175, and COM-NA27RA0173.

## APPENDIX

### Echo Core Variable Definitions

At time of first echo:

FEHtp10 - Top height defined by 10-dBZ contour (km)
FEHMxZ - Height of the core peak reflectivity (km)
FEHbs10 - Base height (km)
FEtpTmp - Top temperature (C°) derived from 0700 CDT PIA sounding
FEmzTmp - Temperature (C°) of core peak reflectivity height derived from 0700 CDT PIA sounding
FEbsTmp - Base temperature (C°) from 0700 CDT PIA sounding
FEA10 - Maximum horizontal area ($km^2$)
FEdpth10 - Depth of the core (km)
FEMxZ - Maximum reflectivity within the core (dBZ)

At time of treatment, radar derived variables:
CPmndia - Mean core diameter (km)
CPHtp10 - Top height (km)
CPMxZ - Peak reflectivity (dBZ)
FECPt - Core age (min)
V_cdp - Vertical growth defined by 10-dBZ contour ($ms^{-1}$)

At time of treatment, aircraft variables near -10°C[1]:
Mean_VW - Updraft speed ($ms^{-1}$)
UP_dia - Updraft diameter (km)
SWC_frac - Fraction of total condensate that was frozen
LWCd - Liquid water content in drizzle and raindrop size distribution ($gm^{-3}$)
NBuoy - Net buoyancy (°C) (= mean thermal buoyancy - loading from liquid water - loading from ice)
Buoy_Enh - Buoyancy enhancement (°C)

Between time of first echo and treatment:
CPFEdH10 - Change in top height (km)
CPFEdA10 - Change in maximum area ($km^2$)
CPFEdZ - Change in peak reflectivity (dBZ)
CPFEdAdt - Rate of change of maximum area ($km^2$ $min^{-1}$)
CPFEdZdt - Rate of change of peak reflectivity (dBZ $min^{-1}$)

At time of the Maximum value:
MaxH10 - Maximum top height (km)
MaxA10 - Maximum area ($km^2$)
MaxZ - Maximum reflectivity (dBZ)
FEMXtMxA - Age of core at maximum area (min)

Between treatment and maximum value:
MXCPdH10 - Change in top height (km)
MXCPdA10 - Change in maximum area ($km^2$)
MXCPdZ - Change in peak reflectivity (dBZ)
CPMXtMxA - Time from treatment to maximum area (min)
V_aft - Vertical growth 4 min following treatment ($ms^{-1}$)
MXCPdAdt - Rate of change in maximum area ($km^2$ $min^{-1}$)
MXCPdZdt - Rate of change in peak reflectivity (dBZ $min^{-1}$)

[1] Changnon, S.A., R.R. Czys, K.R. Gabriel, M.S. Petersen, R.W. Scott, 1993: Results from the 1989 exploratory cloud seeding experiment in Illinois, Annual Report for the Precipitation Cloud Changes, and Impacts Project, Illinois State Water Survey, Champaign, 110 pp.

## 7. REFERENCES


Biondini, R., J. Simpson, and W.L. Woodley, 1977: Empirical predictors for natural and seeded rainfall in the Florida Area Cumulus Experiment (FACE), 1970-1975. *J. Appl. Meteor.*, **16**, 585-594.

Bluestein, H.B., and M.H. Jain, 1985: Formation of mesoscale lines of precipitation: severe squall lines in Oklahoma during the spring. *J. Atmos. Sci.*, **42**, 1711-1732.

Braham, R.R., Jr., 1981: Urban Precipitation Processes, Chapter 3 of METROMEX: A Review and Summary. *Meteorological Monograph.* **18**, American Meteor. Soc., Boston, 75-116.

Braham, R.R., Jr., 1979: Field experimentation in weather modification. *J. Amer. Statis. Assoc.*, **74**, 57-104.

Braham, R.R., Jr., 1966: Final Report of Project Whitetop: Part I -Design of the Experiment; Part II - Summary of Operations. The University of Chicago, 156 pp.

Braham, R.R., Jr., and D. Wilson, 1978: Effects of St. Louis on convective cloud heights. *J. Appl. Meteor.*, **17**, 587-592.

Changnon, S.A., Jr., 1980: Evidence of urban and lake influences on precipitation in the Chicago area. *J. Appl. Meteor.*, **19**, 1137-1159.

Changnon, S.A., Jr., 1978a: Urban effects on severe local storms at St. Louis. *J. Appl. Meteor.*, **17**, 578-586.

Changnon, S.A., 1978b: Vertical characteristics and behavior of radar echoes. In Summary of METROMEX, Vol. 2: Causes of Precipitation Anomalies, SWS Bulletin 63, Illinois State Water Survey, Champaign, Illinois, 274-279.

Changnon, S.A., Jr., 1977: Studies of Urban Effects on Hail Characteristics in METROMEX. In Summary of METROMEX, Volume 1: Weather Anomalies and Impacts, ISWS Bulletin 62, Illinois State Water Survey, Champaign, Illinois, 142-174.

Changnon, S.A., R.R. Czys, M.S. Petersen, R.W. Scott and N.E. Westcott, 1993: Precipitation Cloud Changes and Impacts Project (PreCCIP): Results from the 1989 Exploratory Cloud Seeding Experiment in Illinois, Illinois State Water Survey, Champaign, Illinois, 110 pp.

Changnon, S.A., R.R. Czys, R.W. Scott and N.E. Westcott, 1991: The Illinois precipitation modification program. Bull. Amer. Meteor. Soc., 17, 587-592.

Changnon, S.A., D. Brunkow, R.R. Czys, A. Durgunoglu, P. Garcia, S.E. Hollinger, F.A. Huff, H.T. Ochs, R.W. Scott and N.E. Westcott, 1987: Precipitation Augmentation for Crops Experiment:Phase II, Exploratory Research, Year 1. NOAA NA-86RAH50060. SWS Contract Rep. 430, Illinois State Water Survey, Champaign, Illinois, 159 pp.

Changnon, S.A., Jr. and G. Morgan, 1976: Design of an experiment to suppress hail in Illinois. ISWS Bulletin 61, Illinois State Water Survey, Champaign, Illinois, 194 pp.

Czys, R.R., S.A. Changnon, M.S. Petersen, R.W. Scott and N.E. Westcott, 1993: The 1989 PACE Data Book. Illinois State Water Survey Miscellaneous Publication 144, 250 pp.

Czys, R.R., S.A. Changnon, M.S. Petersen, R.W. Scott and N.E. Westcott, 1992: Initial results from the 1989 cloud seeding experiment in Illinois, *J. Wea. Mod.*, **24**, 13-18.

Dennis, A.S. and A. Koscielski, 1972: Height and temperature of first echoes in unseeded and seeded convective clouds in S. Dakota, *J. Appl. Meteor.*, **11**, 994-1000.

Dennis, A.S. and A. Koscielski, 1969: Results of a randomized cloud seeding experiment in S. Dak., *J. Appl. Meteor.*, **8**, 556-565.

Dennis, A.S., J.R. Miller Jr., E.I. Boyd and D.E. Cain, 1975: Effects of cloud seeding on summertime precipitation in N.Dak.. Bur. of Rec. Rep. 75-1, S. Dak. School of Mines, Rapid City, 97 pp.

Flueck, J.A., 1971: Final Report of Project Whitetop: Part V -Statistical Analysis for the Ground Level Precipitation Data, The University of Chicago, 294 pp.

Fovell, R.G., and Y. Ogura, 1989: Effects of vertical shear on numerically simulated multicell storm structure. *J. Atmos. Sci.*, **46**, 3144-3176.

Gagin, A., D. Rosenfeld and R. Lopez, 1986: The relationship between height and precipitation characteristics of summertime convective cells in South Florida. *J. Atmos. Sci.*, **42**, 84-94.

Hiser, 1956: Type distribution of precipitation at selected stations in Illinois. Trans. *Amer. Geoph. Union.* **37**, 421-424.

Hudson, H.E., Jr., G.E. Stout, and F.A. Huff, 1952: Studies of thunderstorm rainfall with dense raingage networks and radar. ISWS Report of Investigation 13, Illinois State Water Survey, 30 pp.

Huff, 1969: Climatological assessment of natural precipitation characteristics for use in weather modification. *J. Appl. Meteor.*, **8**, 401-410.

Kennedy, P.C., N.E. Westcott, and R.W. Scott, 1989: Single Doppler radar observations of a mini-tornado. Preprint, 16th Conf. on Severe Local Storms, Kananaskis, Provincial Park, Alta., Canada, 209-212.

LeMone, M.A., 1989: The influence of vertical wind shear on the diameter of cumulus clouds in COPE. *Mon. Wea. Rev.*, **117**, 1480-1491.

Marwitz, J.D., 1972: The structure and motion of severe hailstorms. Part II. Multi-cell storms, *J. Appl. Meteor.*, **11**, 180-188.

Mather, G.K., B.J. Morrison, and G.M. Morgan, Jr., 1986: A preliminary assessment of the importance of coalescence in convective clouds of the eastern transvaal. *J. Appl. Meteor.*, **25**, 1780-1784.

Montcrieff, M.W., and J.S.A. Green, 1972: The propagation and transfer properties of steady convective overturning in shear. *Quart. J. Roy. Meteor. Soc.*, **98**, 336-352.

Newton, C.W., and H.R. Newton, 1959: Dynamical interactions between large convective clouds and environment with vertical shear. *J. Meteor.*, **16**, 483-496.

Orville, H.D., 1986: A review of dynamic mode seedinof summer cumuli. Chapter 6 of Precipitation Enhancement - A Scientific Challenge, Meteor. Mono. 2(43), 43-62.

Peppler, R.A., 1988: A review of static stability indices and related thermodynamic parameters. Illinois State Water Survey Misc. Pub. 104, Champaign, Illinois, 87 pp.

Peppler, R.A., and P.J. Lamb, 1989: Tropospheric static stability and central North American growing season rainfall. *Mon.Wea.Rev.*, **117**,: 1156-1180

Petersen, R., 1984: Triple Doppler radar analysis of discretely propagating multicell convective storms. *J. Atmos. Sci.*, **41**, 2973-2990.

Rosenfeld D., and W.L. Woodley, 1989: Effects of cloud seeding in West Texas. *J. Appl. Meteor.*, **21**, 1050-1080.

Rotunno, R., J.B. Klemp, and M.L. Weisman, 1988: A theory for strong, long-lived squall lines. *J. Atmos. Sci.*, **45**,: 463-485.

Scott, R.R. and R.R. Czys, 1992: Objective forecasting of some individual cloud characteristics in the 1989 PACE cloud seeding experiment. *J. Wea. Mod.*, **24**, 1-12.

Scott, R.W. and F.A. Huff, 1987: PACE 1986 forecasting program -design, operations and assessment. Preprint, 11th AMS Conf. on Wea. Modif., Edmonton, Alta., Canada, 102-105.

Simpson, J., 1980: Downdrafts as linkages in dynamic cumulus seeding effects. *J. Appl. Meteor.*, **19**, 477- 487.

Simpson, J. and W.L. Woodley, 1971: Seeding cumulus in Florida: New 1970 results. *Science*, **172**, 117-126.

Towery, N.G. and S.A. Changnon, Jr., 1970: Characteristics of hail producing radar echoes in Illinois. *Mon. Wea. Rev.*, **98**, 346-353.

Vogel, J.L., 1977: Synoptic Weather Relations. In Summary of METROMEX, Volume 1: Weather Anomalies and Impacts, ISWS Bull. 62, Illinois State Water Survey, Champaign, Illinois, 85-112.

Weisman, M.L., and J.B. Klemp, 1984: The structure and classification of numerically simulated convective storms in directionally varying wind shears. *Mon. Wea. Rev.*, **112**, 2479-2498.

Weisman, M.L., and J.B. Klemp, 1982: The dependence of numerically simulated convective storms on vertical wind shear and buoyancy. *Mon. Wea. Rev.*, **110**, 504-520.

Weisman, M.L., J.B. Klemp, and R. Rotunno, 1988: Structure and evolution of numerically simulated squall lines. *J. Atmos. Sci.*, **45**, 1990-2013.

Westcott, N.E., 1990: Radar results of the 1986 Exploratory field program relating to the design and evaluation of PACE. *J. Wea. Mod.*, **22**, 1-17.

Westcott, N.E., and P.C. Kennedy, 1989: Cell development and merger in an Illinois thunderstorm observed by Doppler radar. *J. Atmos. Sci.*, **46**, 117-131.